DTIC FILE COPY

SECURITY CLASSIFICATION OF THIS PAGE

REPORT DOCUMENTATION PAGE

Form Approved OMB No. 0704-0188

1a. REPORT SECURITY CLASSIFICATION UNCLASSIFIED	1b. RESTRICTIVE MARKINGS NONE
2a. SECURITY CLASSIFICATION AUTHORITY AD-A218 249	3. DISTRIBUTION/AVAILABILITY OF REPORT APPROVED FOR PUBLIC RELEASE; DISTRIBUTION UNLIMITED.
	5. MONITORING ORGANIZATION REPORT NUMBER(S) AFIT/CI/CIA-89-023
6a. NAME OF PERFORMING ORGANIZATION AFIT STUDENT AT Univ of Minnesota	6b. OFFICE SYMBOL (If applicable)
	7a. NAME OF MONITORING ORGANIZATION AFIT/CIA
6c. ADDRESS (City, State, and ZIP Code)	7b. ADDRESS (City, State, and ZIP Code) Wright-Patterson AFB OH 45433-6583
8a. NAME OF FUNDING/SPONSORING ORGANIZATION	8b. OFFICE SYMBOL (If applicable)
	9. PROCUREMENT INSTRUMENT IDENTIFICATION NUMBER
8c. ADDRESS (City, State, and ZIP Code)	10. SOURCE OF FUNDING NUMBERS

PROGRAM ELEMENT NO.	PROJECT NO.	TASK NO.	WORK UNIT ACCESSION NO.

11. TITLE (Include Security Classification) (UNCLASSIFIED)
Infrared and X-ray Photoelectron Spectroscopy Studies of the Polyimide/Metal Interface

12. PERSONAL AUTHOR(S)
William Creed Stewart

13a. TYPE OF REPORT	13b. TIME COVERED	14. DATE OF REPORT (Year, Month, Day)	15. PAGE COUNT
THESIS/~~DISSERTATION~~	FROM _____ TO _____	1989	115

16. SUPPLEMENTARY NOTATION
APPROVED FOR PUBLIC RELEASE IAW AFR 190-1
ERNEST A. HAYGOOD, 1st Lt, USAF
Executive Officer, Civilian Institution Programs

17. COSATI CODES			18. SUBJECT TERMS (Continue on reverse if necessary and identify by block number)
FIELD	GROUP	SUB-GROUP	

19. ABSTRACT (Continue on reverse if necessary and identify by block number)

DTIC
ELECTE
FEB 15 1990
S D
D

90 02 14 074

20. DISTRIBUTION/AVAILABILITY OF ABSTRACT	21. ABSTRACT SECURITY CLASSIFICATION
☒ UNCLASSIFIED/UNLIMITED ☐ SAME AS RPT. ☐ DTIC USERS	UNCLASSIFIED

22a. NAME OF RESPONSIBLE INDIVIDUAL	22b. TELEPHONE (Include Area Code)	22c. OFFICE SYMBOL
ERNEST A. HAYGOOD, 1st Lt, USAF	(513) 255-2259	AFIT/CI

DD Form 1473, JUN 86 *Previous editions are obsolete.* SECURITY CLASSIFICATION OF THIS PAGE

AFIT/CI "OVERPRINT"

INFRARED AND X-RAY PHOTOELECTRON SPECTROSCOPY STUDIES OF THE POLYIMIDE / METAL INTERFACE

A THESIS

SUBMITTED TO THE FACULTY OF THE GRADUATE SCHOOL

OF THE UNIVERSITY OF MINNESOTA

BY

WILLIAM CREED STEWART

IN PARTIAL FULFILLMENT OF THE REQUIREMENTS

FOR THE DEGREE OF

MASTER OF SCIENCE IN CHEMICAL ENGINEERING

APRIL 1989

ABSTRACT

This thesis considers the chemical interactions which occur at the interface of a polymer and a metal. Polyimides were chosen for this study because of their application in microelectronic devices, flexible interconnects, solar cells, and printed circuit boards. In these applications polyimide typically forms an interface with chromium, aluminum, copper, or gold. Numerous results have been published on the processes which occur when metals are deposited on cured polyimide. Less attention has been given to the equally important sequence of polyimide curing on a metal.

The interfaces studied for this thesis were those formed by imidization of polyamic acid on gold, chromium, and copper. Infrared spectroscopy (IR) and x-ray photoelectron spectroscopy (XPS) were used to study these interfaces. Polyimide films as thin as 34 Å were prepared on metallized silicon wafers for these analyses. Attenuated total reflection and reflection/absorption techniques were used to collect the infrared spectra of these thin films.

The IR and XPS results indicated the gold interacted very little with the polyimide, while copper produced significant changes in the IR and XPS spectra. At elevated cure temperatures chromium also reacted with the polyimide. In the structures with chromium and copper, the thermal stability of the polyimide at the interface was reduced from that of bulk polyimide. The data showed that the metals interact with the polymer structure at the point where ring closure occurs to form the polyimide from polyamic acid.

The data presented in this thesis, particularly the infrared spectra, add significant information to the chemical characterization of the polyimide/metal interface and the processes which occur during its formation.

ACKNOWLEDGEMENTS

I would like to express my gratitude to the United States Air Force for sponsoring my graduate studies at the University of Minnesota and to my advisor, Professor Klavs Jensen, for his guidance throughout my research. Access to data acquisition capabilities provided by an IBM Materials Science and Processing Grant is appreciated.

Thanks also go to Craig Schuckert of Dupont for supplying the polyimide and to Tom Ritzdorf of Control Data Corporation for preparing the copper metallizations. Jihperng Leu's assistance with the FTIR is gratefully acknowledged, as well as the discussions with Dr. Raul Caretta concerning the XPS studies.

Most of all I thank my family and friends who supported and encouraged me throughout my studies. Thank you Sherri, David, and James for your love, patience, and understanding. This is as much yours as it is mine.

TABLE OF CONTENTS

Chapter	Title	Page
1	**Introduction**	1
2	**Analytical Techniques**	6
	Introduction	6
	Infrared Spectroscopy	7
	X-ray Photoelectron Spectroscopy	16
3	**Polyimide Chemistry, Characterization and Properties**	22
	Polyimide Chemistry	22
	Infrared Spectroscopy Characterization	26
	X-ray Photoelectron Spectroscopy Characterization	33
4	**Background Information on Polyimide/Metal Interfaces**	40
	Introduction	40
	Copper-Polyimide Interface	41
	Gold-Polyimide Interface	44
	Aluminum-Polyimide Interface	45
	Chromium-Polyimide Interface	49
	Titanium-Polyimide Interface	54
5	**Experimental Procedures**	56
	Introduction	56
	Test Structure Configuration	56
	Test Structure Fabrication	59
	Metallization Process	59
	Polyimide Application	61
	Infrared Spectroscopy	65
	X-ray Photoelectron Spectroscopy	66
6	**Experimental Results**	69
	Introduction	69
	Polyimide Characterization	69
	Polyimide-Gold Interface	76
	Polyimide-Chromium Interface	80
	Polyimide-Copper Interface	84
	Cure Temperature Effect	93
	Summary	94
7	**Conclusions and Recommendations**	99

CHAPTER 1

INTRODUCTION

While a wide variety of polymer and metal interfaces are present in electronic and aerospace systems, problems related to the chemical and physical nature of the interface remain to be understood. As applications having such interfaces continue to increase, it becomes increasingly important to system performance and reliability to understand the process of forming a polymer/metal contact.

Polyimides are the class of polymers chosen for this study because of their use in microelectronic devices, flexible interconnects, solar cells, printed circuit boards, aerospace composites, and adhesives. The properties of polyimides which make them desirable for such applications are high thermal stability, low dielectric constant, a high bulk resistivity, planarizing capability, and ability to apply with low defect density. The technological importance of polyimides can be seen by considering a few specific applications.

The widest, and perhaps the fastest growing, use of polyimides is for very large scale integrated (VLSI) and very high speed integrated (VHSIC) circuits.[1] While the electrical properties of polyimide are comparable to those of silicon dioxide[2], the most widely used insulating layer, polyimide possesses processing and planarizing advantages.[3,4] The ability to obtain planarized layers is critical in the multilevel metallization processes of these technologies where topography of metal edges and via holes for interlayer interconnections impact device reliability and yield.[5,6,7,8] In these

cases polyimide forms an interface with a conductor of aluminum or aluminum/copper alloy. IBM is currently using a polyimide dielectric in devices being fabricated for the Department of Defense Tri-Service VHSIC Program.[9]

A similar application, but at the device packaging level, is an effort to develop a high speed package for digital GaAs devices operating at speeds above 3 GHz.[10,11] The package is a multilevel structure consisting of copper conductors imbedded in polyimide dielectric to provide the high speed signal transmission.

Because polyimide is tough, resilient, and can be applied with a low defect density, it has been used as a protective overcoat on integrated circuits and solar cells. In addition, the overcoat can protect against nondestructive soft error problems in charge coupled devices and dynamic memories caused by alpha radiation emitted by trace amounts of thorium and uranium present in packaging materials.[12,13] Several memories produced to MIL-M-38510 requirements now use polyimide to prevent these soft errors.

Photoimagable polyimide systems are also receiving increased attention by the integrated circuits industry.[14] These polyimide systems could be applied and patterned like a photoresist but remain as a permanent part of the device structure. The direct result is a reduction in the required processing steps.

The aerospace community has shown increased interest in polyimide materials for aerospace composites and adhesives as the time/temperature performance of advanced materials are driven by programs like the Space Shuttle, the Advanced Tactical Fighter, and

the National Aerospace Plane.[15] The National Aeronautics and Space Administration has been the pioneer in this area, and has successfully demonstrated applications with several NASA programs and joint efforts with Army, Navy , and Air Force programs.[16]

The above examples clearly show the technological importance of polyimides in electronic and aerospace industries. The successful application of this novel class of polymers will require an increased understanding of the chemical and physical processes which occur at the interface of polyimides and metals, since the formation of chemical bonds can give rise to an eight-fold increase in intrinsic adhesion across interface.[17]

While several papers have been published by researchers looking at the *in situ* deposition of metals onto polyimide films, much less attention has been given to the equally important process of curing polyimide on a metal. The *in situ* experiments have used x-ray photoelectron spectroscopy (XPS) to analyze the chemical changes occurring at the interface and transmission electron microscopy to study the morphological changes.

This thesis will study the interface obtained when polyamic acid is imidized on a metal film. Infrared (IR) analysis and XPS were the analytical techniques used. The test structures were prepared by spin-coating the polyamic acid precursor to polyimide onto metallized wafers, with film imidization conducted in nitrogen. The IR and XPS results were considered in light of previously published data. The work considered differences in interfaces caused by cure conditions, by different metals, and by process sequence.

REFERENCES

[1]G. Samuelson, "Polyimide for Multilevel Very Large-Scale Integration," *Polymer Materials for Electronic Applications*, edited by E.D. Feit and C.W. Wilkins, Jr., ACS Symposium Series 184, American Chemical Society, 93-106 (1982).

[2]A.M. Wilson, "Use of Polyimides in VLSI Fabrication," *Polyimides: Synthesis, Characterization, and Applications*, edited by K.L. Mittal, 715-733, Plenum Press (1984).

[3]D.R. Day, D. Ridley, J. Mario, and S.D. Senturia, "Polyimide Planarization in Integrated Circuits," *Polyimides: Synthesis, Characterization, and Applications*, Edited by K.L. Mittal, 767-781, Plenum Press (1984).

[4]C.C. Chou and W.V. Wang, "Planarization Enhancement of Polyimides by Dynamic Curing and the Effect of Multiple Coating," *Polyimides: Synthesis, Characterization, and Applications*, Edited by K.L. Mittal, 783-793, Plenum Press (1984).

[5]K. Mukai, A. Saiki, K. Yamanaka, S. Harada, and S. Shoji, "Planar Multilevel Interconnection Technology Employing a Polyimide," *IEEE J. Solid State Circuits*, **SC-13 (4)**, 462-467, August 1978.

[6]P. Shah, D. Laks, and A. Wilson, "High Performance, High Density MOS Process Using Polyimide Interlevel Insulation," *IEEE Proceedings EDM 79*, 465-468, December 1979.

[7]T. Nishida, A. Saiki, Y. Homma, and K. Mukai, "Advanced Planar Metallization With Polymer for VLSI,"*IEEE Proceedings IEDM 82*, 552-555 (1982).

[8]A.J.P. Theuwissen and G.J. Declerck, "Linear CCD-Imagers with a Polyimide Insulation for Double Level Metallization," *IEEE Electron Device Letters*, **EDL-3 (10)**, 308-309, October 1982.

[9]IBM/Federal Systems Division, Manassas, VA. Contract No. N0039-81-C-0416, Naval Electronics Systems Command, Washington, DC.

[10]R.J. Jensen, J.P. Cummings, and H. Vora, "Copper/Polyimide Materials System for High Performance Packaging," *IEEE Transactions on Components, Hybrids, and Manufacturing Technology*, **CHMT-7 (4)**, 384-393, December 1984.

[11]R. Sainati, Honeywell Physical Sciences Center, Bloomington, MN. Contract No. F30602-85-C-0054, Rome Air Development Center, Griffiss AFB, NY.

[12]Y.K. Lee and J.D. Craig, "Polyimide Coatings for Microelectronic Applications," *Polymer Materials for Electronic Applications*, edited by E.D. Feit and C.W. Wilkins, Jr., ACS Symposium Series 184, American Chemical Society, 107-121(1982).

[13]Notes from Polymer Materials for Electronic Applications short course. University of California-Berkeley, 16-17 August 1983.

REFERENCES (continued)

[14]J. Pfeifer and O. Rohde, "Direct Photoimaging of Fully Imidized Solvent-Soluable Polyimides,"*Recent Advances in Polyimide Science and Technology*, Edited by W.D. Weber and M.R. Gupta, 336-350, The Mid-Hudson Chapter of The Society of Plastics Engineers, Inc. (1987).

[15]A.K. St. Clair and T.L. St. Clair, "The Development of Aerospace Polyimide Adhesives," *Polyimides: Synthesis, Characterization, and Applications*, Edited by K.L. Mittal, 977-1002, Plenum Press (1984).

[16]T.T. Serafini, "PMR Polyimide Composites for Aerospace Applications," *Polyimides: Synthesis, Characterization, and Applications*, Edited by K.L. Mittal, 957-975, Plenum Press (1984).

[17]N.J. Chou and C.H. Tang, "Interfacial Reaction During Metallization of Cured Polyimide: An XPS Study," *J. Vac. Sci. Technol.* **A2 (2)**, 751-755 (1984).

CHAPTER 2

ANALYTICAL TECHNIQUES

INTRODUCTION

Infrared spectroscopy (IR) and x-ray photoelectron spectroscopy (XPS), also known as electron spectroscopy for chemical analysis (ESCA) were used to study the polyimide/metal interfaces. Figure 2-1 shows the electromagnetic spectrum, along with the type of energy-level transitions which occur as the radiation interacts with an atom or molecule.[1]

Figure 2-1. Electromagnetic Spectrum

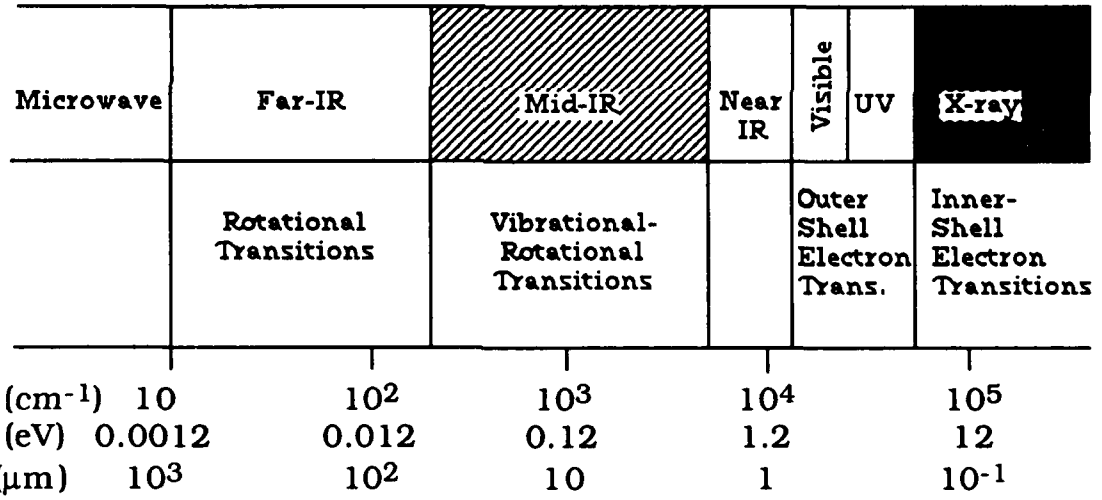

IR is associated with the rotational and vibrational energy transitions which occur in the 400-5000 cm^{-1} (0.05-0.63 eV). In order for a molecule to have an IR spectrum, it must have a permanent dipole moment and must vibrate about a bond or rotate about an axis perpendicular to the bond. These characteristics make IR useful for

characterizing organic materials. Infrared data is typically reported as radiation wavelength (λ) in μm or wavenumber ($\bar{\nu}$) in cm^{-1}. Wavelength and wavenumber are related by

$$\bar{\nu} = \frac{1}{\lambda}$$

Since x-rays are higher energy radiation than IR energy, the x-rays interact with the interior electrons of an atom. As a result of the impinging high-energy x-rays, several inner shell electronic transitions produced. XPS characterizes a material by analyzing the transition which occurs when electrons are emitted from the material. XPS data is typically reported in energy units of electronvolt (eV). The energy (E) of the electromagnetic radiation is related to its wavelength and wavenumber by

$$E = \frac{hc}{\lambda} = (hc)\,\bar{\nu}$$

where

h= Planck's constant (6.67×10^{-27} erg-sec)

c= velocity of light (3×10^{10} cm/sec).

(Note: 1 eV = 1.6×10^{-12} erg).

Infrared Spectroscopy

In general terms, infrared analysis is conducted by passing radiation given off by a source through a sample and recording the ratio of the result to that of the source energy unattenuated by sample absorbances. As shown in Figure 2-1, the absorption bands which appear result from the interaction of the radiation with the specific vibrational-rotational energy-level transitions of that molecule.

In Fourier transform infrared spectroscopy (FTIR), a broad region of IR energy is measured simultaneously by recording an interferogram, an interference pattern generated when a beam of light is divided and recombined after a path difference has been introduced. A Fourier transform is used to convert the interferogram into a spectrum. Spectra must be acquired for both the sample and a reference, either concurrently or sequentially.[2] The sample and reference spectra are ratioed to produce a transmittance or absorbance spectrum, where

$$\text{Transmission} = \frac{\text{Sample}}{\text{Reference}}$$

and

$$\text{Absorbance} = -\log \frac{\text{Sample}}{\text{Reference}}$$

A wide range of sampling techniques have been used to optimize the IR information available from a given type of sample (i.e., solid, liquid, gas) or geometry. While transmission techniques are the simplest to setup, calibrate, and obtain repeatable results from, these techniques to not accommodate all possible materials or configurations from which IR data may be desired. As a result novel techniques have been which are useful for studying the surfaces of polymers and the interfacial reactions which occur between polymers and other materials. Of particular interest are external and internal reflection techniques.

The external reflection technique, typically referred to as reflection-absorption (RA), is useful for samples where a material interfaces with a metal. As a result a reflecting surface is built into the

film/metal structure, and IR spectra of surface species and thin films can be obtained by reflection from the metal surface. Figure 2-2 shows a RA configuration utilizing a single reflection.

Figure 2-2. Single Reflection RA Configuration

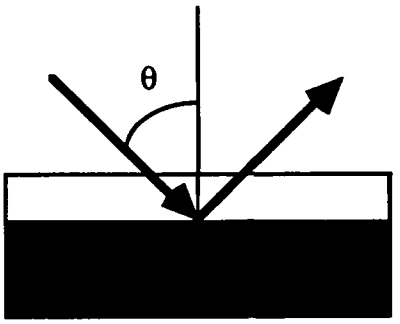

When a metal surface is irradiated with IR energy, an electric field is created near the surface. The magnitude of the electric field and the resulting IR spectrum is a function of impinging radiation's angle of incidence and polarization.

The perpendicular-polarized (s-polarized) component of the light has a phase shift of 180° at all angles of incidence. As a result, a standing wave with a node close to the reflective surface is established. Since this low amplitude radiation is unable to interact with the thin film or surface species, s-polarized radiation does not contribute to the IR spectrum.

The parallel-polarized (p-polarized) component has zero phase shift from normal incidence (θ=0°) to near grazing incidence, at which point the phase shift rapidly changes and approaches 180°. When a phase shift less than change 180° occurs, the electric field at the

reflecting surface has a significant component perpendicular to the surface. Since the p-polarized radiation has a finite amplitude, it can interact with the surface species up to incident angles very close to 90°. Only dipole moments of surface species perpendicular to the reflective surface interact with the electric field.

Because of the characteristics of the established electric fields, little interaction occurs between the sample and the radiation at normal incidence. The interaction increases for p-polarized light (or light with a p-polarized component) up to θ=88°, the incident angle at which maximum interaction occurs. The 88° incident angle is experimentally difficult to use, so typical angles fall into the 75° to 85° range.[3]

Since the p-polarized light interacts with species perpendicular to the incident plane, polarization studies are useful for determining molecular orientation or crystallinity in films and fibers. Although RA studies offer this unique capability, RA experimental configurations are more often selected due to high sensitivity.

An IR spectrum obtained by RA can be 10 to 50 times stronger than a corresponding transmission spectrum.[3] The following equation relates the thickness of films required by RA and transmission to yield IR spectra with equal intensities:[2]

$$d_{RA} = d_{TR} \frac{\cos \alpha}{2}$$

where

d_{RA}= thickness of RA film

d_{TR} = thickness of transmission film

θ= angle of incidence with respect to surface normal

That is, the RA film thickness required to produce the same intensity absorbance band decreases with increasing angle of incidence.

One disadvantage of the RA technique is that frequency shifts of the IR absorbance bands occur. Broad absorption bands are shifted much more than narrow bands, with bands always shifted to higher frequencies for very thin films. The shifts are also a function of the angle of incidence.[3]

IR accessories are available which permit multiple reflection sampling, with the distance between the reflecting surfaces controlling the number of reflections. The number of reflections is given by

$$N = \frac{\tan \theta}{t}$$

where

N= number of reflections

θ= angle of incidence with respect to surface normal

t= distance between reflecting surfaces (equivalent to internal reflection element thickness)

Multiple reflections increase signal strength; however, the reflections in RA are not loss-less. Since the background decreases with each reflection, an infinite number of reflections is not optimal. While it is possible to optimize the signal-to-noise ratio of an IR spectrum with

multiple RA, the gains must be weighed against increased sample constraints and alignment problems. For example, roughly equal sample sizes are required for 10 reflections at 45° and 1 reflection at 85°. However, since cos 45° is roughly 10 times greater than cos 85°, the measured absorbance would be about the same.[2] In general, single reflection absorbance bands are greater than 60% of the optimum value attainable with multiple RA.[3]

In internal reflection spectroscopy, commonly called attenuated total reflection (ATR) spectroscopy, IR radiation is passed through a crystal with a high refractive index and impinges on a flat interface with a sample having a lower refractive index.[4,5] The crystal is referred to as the internal reflection element (IRE). This set-up is shown in Figure 2-3. The advantage ATR has over RA is that it can be used to study any sample which can be brought into contact with an IRE and interacts with IR radiation.

Figure 2-3. Multiple Reflection ATR Configuration With Fixed-Angle, Single-Pass Plate

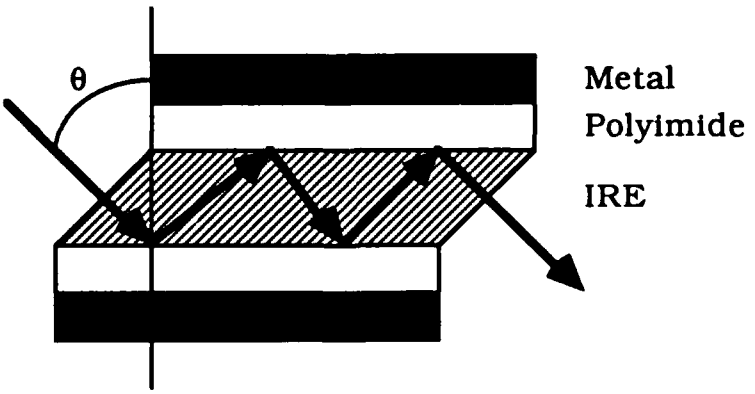

The radiation propagating in an IRE undergoes total reflection at the interface when the angle of incidence exceeds the critical angle defined by

$$\theta_c = \sin^{-1} \frac{n_s}{n_r} = \sin^{-1} n_{sr}$$

where

θ_c= critical angle

n_s= refractive index of sample

n_r= refractive index of IRE, ($n_r > n_s$)

$$n_{sr} = \frac{n_s}{n_r}$$

Unlike external reflection, the reflectivity for internal reflection is 100% when $\theta > \theta_c$.[4]

As a result of the total reflection, a standing wave is established in the IRE normal to the interface, and an evanescent, nonpropagating field is established in the sample. The evanescent field is a nontransverse field and has components in all directions. Parallel to the surface is a nonzero energy flow which produces displacement of the incident and reflected waves.[4,5]

If a nonabsorbing sample is used, the normal component of energy flow into it must be zero in order for total reflection to occur (i.e., no energy loss). However, if an IR absorbing material is sampled, the evanescent wave interacts with it and attenuates the IR signal propagating in the IRE, producing an IR spectrum. Compared to the energy lost with external reflection to the metal reflector, ATR is relatively loss-less. When systems are well-designed and IRE's are properly cared for, the energy remains constant regardless of the

number of reflections. As a result multiple reflections can enhance very weak absorption bands.

The evanescent field is confined to the region near the surface of the sample, and its amplitude decays exponentially with distance into the sample (i.e., normal to the interface). The penetration depth of the evanescent wave has been defined as the distance at which the field is diminished to $1/e$ of its value at the IRE/sample interface. The penetration depth is given by[2,3,4,5]

$$d_p = \frac{\lambda}{2 \pi n_r \sqrt{\sin^2\theta - n_{sr}^2}}$$

where the symbols are those previously defined. Several important observations can be made from this equation. First, d_p increases linearly with λ, producing distorted bands at longer wavelengths. Also, d_p can be lowered for a given film either by increasing θ or by using a different IRE with a higher n_r. The maximum penetration depth occurs at θ_c.[3,4] Experimentally, it has been found that the actual depth sampled is about three times the defined penetration depth.[5] This is not surprising since by definition the electric field still has 37% of its surface value at d_p.

IRE's are available in many geometries fabricated from a variety of materials. The type of sample to be studied and the IR region of interest quickly narrow the choices. The possible geometries of an IRE are too numerous to list, but a few of the variables will suffice to show the extent of possibilities: single- or multiple-reflections; fixed- or variable-angle; single- or-double pass; prism, plate, hemisphere, hemicylinder, rod, or some other shape. A few standard elements,

however, like the multiple-reflection, fixed-angle, single-pass plate shown in Figure 2-3, are used in most applications. This plate is particularly useful for very thin films and surface studies.[4]

For the mid-IR region, silicon, germanium, gallium arsenide, and KRS-5 are typical choices due to their transparency over a wide range. KRS-5, the double salt of thallium bromide and thallium iodide, is possibly the most common material since it is transparent from 14,000 cm^{-1} to 350 cm^{-1}. Silicon is useful in mid-IR only to 1670 cm^{-1}, while germanium is useful to 875 cm^{-1}. GaAs is good to 715 cm^{-1}.[4,6] KRS-5 also offers a lower refractive index than the other materials, which is useful for thin film analysis where one does not need to be concerned with distortions caused by thick films.[4]

KRS-5 is soft, which can be advantage when trying to obtain good optical contact with hard, rough materials. The softness, however, can become a disadvantage since the material can be easily scratched, bent, or deformed. Marred and/or dirty IRE surfaces result in significant energy losses and distortions.

Optical contact for solid samples is obtained by holding the sample against the IRE with a back plate under pressure from a screw clamp. Since pressure changes can change absorption characteristics, tightening of the clamp must be controlled in a repeatable manner. Other variables which impact the reproducibility of IR spectra may be obtained are the sample homogeneity, sample position on the IRE, and area of IRE coverage.

X-ray Photoelectron Spectroscopy

XPS uses monoenergetic soft x-rays to excite electron emission from the core levels of an atom. Since each element has a specific electronic structure, the energies of the emitted electrons (photoelectrons) are unique to the element and its oxidation state. The characteristic binding energy of the emitted electrons is obtained from the following equation:[7]

$$E_B = h\nu - E_K - \phi$$

where

E_B = electron binding energy of photoelectron

E_K = kinetic energy of photoelectron

$h\nu$ = photon energy, where ν is radiation frequency

ϕ = work function

Because each atom has a variety of possible ions, there is a corresponding set of discrete energetic photoelectrons emitted. However, each element has a characteristic band which is most intense and, therefore, most suitable for identifying chemical states.

In addition to the photoelectron, Auger electrons are normally emitted during the photoionization process. The Auger electron results from an outer shell electron falling in to the inner shell vacancy created by the photoionization. A second electron, the Auger electron, is emitted to carry off the excess energy and has a kinetic energy equal to the difference between the energy of the initial ion and the final doubly charged ion. Since each element has a specific electronic structure yielding specific ions from photoionization, each

element has a characteristic Auger spectrum which is independent of the initial ionization mode.

In practice, the electrons which leave a surface are detected by an electron spectrometer which analyzes the electrons according to kinetic energy. Samples with unknown composition are typically scanned for binding energies ranging from 1000-0 eV. Based upon element identifications made from the survey spectrum, detail scans of specific regions are then run for chemical state identification, quantitative analysis, or mathematical analysis of the bands. Regions which may be radiation sensitive should be run first.[8]

An XPS analysis provides a chemical analysis limited to the top 20 to 50 Å of a surface.[9]. Although the path length of the photons is in the micrometer range, the escape depth of the photoelectrons is in the angstrom range. In other words, ionization occurs to a depth of a few micrometers, but only electrons generated within the top few angstroms can escape the surface. Theoretical and experimental data indicate the electron mean free path (λ) is only subtly dependent upon the material. As a result, λ for a given kinetic energy falls within a narrow range for materials with very different electronic structures.[10] Empirical data [8] shows λ is proportional to $(E_K)^{0.75}$.

A simple schematic of the typical geometry of an XPS analysis is shown in Figure 2-4. Common x-ray sources are magnesium and aluminum, which emit Kα x--rays at 1253.6 eV and 1486.6 eV,

Figure 2-4. Typical XPS Spectrometer Configuration

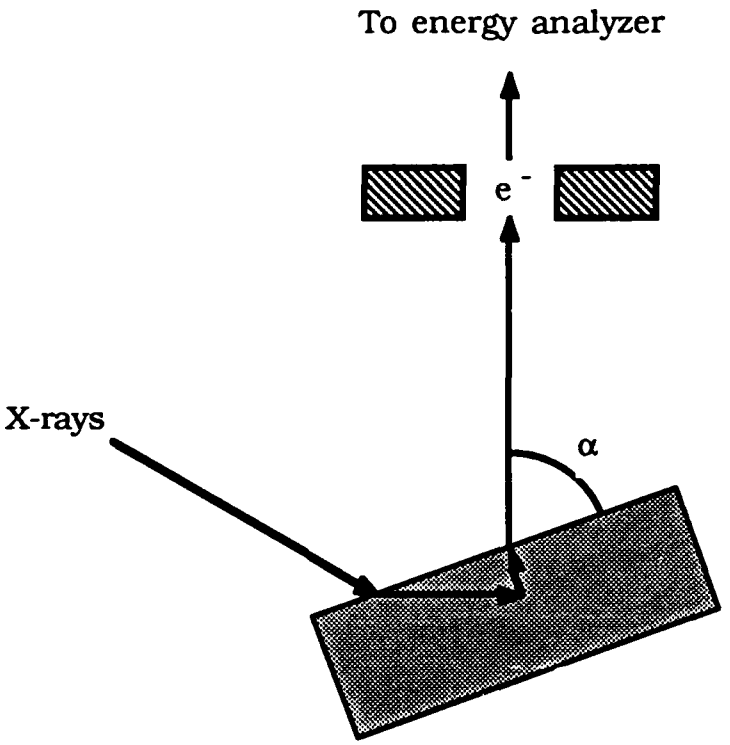

respectively. Magnesium provides slightly better band resolution due to a smaller x-ray line width, while aluminum analyzes slightly deeper due to its higher energy x-rays. Most commercial instruments have a dual anode capability. Since photoelectron energies are determined by the exciting photon energy, while Auger electron energies are fixed, a change in the x-ray line energy can resolve interferences in an XPS spectrum.[7]

The most common types of electron energy analyzers are the cylindrical mirror analyzer and concentric hemispherical analyzer (CHA). Both analyzers are dispersive analyzers, which utilize a deflecting electrostatic field to disperse the electron energies so that

at any given time only energies within narrow range are measured. Scanning the applied potential gives the energy distribution of the electrons passing through it. Retardation grids or lenses are used to improve the energy resolution of the analyzer.[7]

The CHA is the most common analyzer for XPS because it can maintain adequate luminosity with high resolution and is better suited for angular dependence measurements due to a narrower acceptance angle. The CHA can be operated in two retarding modes: constant relative resolution (CRR) or constant absolute resolution (CAT). In the CRR mode electrons are decelerated by a constant ratio, resulting small peaks at low kinetic energies being more easy detect. In the CAT mode electrons are decelerated to a constant pass energy. The CAT mode is easier for quantification, but has poorer signal-to-noise characteristics at low kinetic energies.[7]

Experimental XPS bands often consist of several overlapping peaks of different shapes and intensities. Two main methods for isolating and defining these individual contributions are deconvolution and curve fitting, but neither can provide a unique solution to the problem.[11]

Deconvolution refers to a method of obtaining the "true" spectrum (f_t) from the "observed" spectrum (f_o) by compensating for instrumental factors like the resolving power of the spectrometer and the x-ray line width. Mathematically the relation is represented by

$$f_o = f_t B$$

where B is the function incorporating the instrumental factors. Successful deconvolution depends upon having good raw data with which to work.

Curve fitting uses a series of functions representing individual components in order to produce a final function which is close to the experimental XPS band. The process is very dependent on initial guesses such as the number of components contributing to the experimental band and the component parameters. Each individual peak has the following parameters which must be considered: position of the peak center; peak intensity; peak width; peak shape or function type; and peak tail characteristics. The most common type of function used for curve fitting is a mixed Gaussian/Lorentzian. Essentially any peak shape may be synthesized by varying the Gaussian/Lorentzian mixing ratio and the tail parameters.[11] In order to optimize the curve synthesis procedure, the nonlinear least squares method has been incorporated into to the process. The statistical information available from this process helps in determining the "best fit" of the experimental data. However, a given fit is not unique, and is dependent upon the initial parameter inputs. A "best fit" decision must be based upon statistical information which is consistent with known chemical and spectroscopic data.

REFERENCES

[1]N.L. Alpert, W.E. Keiser, and H.A. Szymanski, *IR: Theory and Practice of Infrared Spectroscopy*, Plenum Press (1970).

REFERENCES (continued)

[2]P.R. Griffiths and J.A. de Haseth, *Fourier Transform Infrared Spectrometry*, John Wiley & Sons (1986).

[3]S.R. Culler, H. Ishida, and J.LO. Koenig, "The Use of Infrared Methods to Study Polymer Interfaces," *Ann. Rev. Mater. Sci*, **13**, 363-386 (1983).

[4]N.J. Harrick, Internal Reflection Spectroscopy, John Wiley & Sons, Inc. (1967).

[5]F.M. Mirabella, Jr., "Internal Reflection Spectroscopy," *Applied Spectroscopy Reviews*, **21(1&2)**, 45-178 (1985).

[6]Harrick IR-VIS-UV Accessories, Catalog HSC-831, Harrick Scientific Corporation, Ossining, NY.

[7]J.C. Riviere, "Instrumentation," *Practical Surface Analysis by Auger and X-ray Photoelectron Spectroscopy*, Edited by D. Briggs and M.P. Seah, John Wiley & Sons, (1983).

[8]C.D. Wagner, W.M. Riggs, L.E. Davis, J.F. Moulder, and G.E. Mullenberg, *Handbook of X-ray Photoelectron Spectroscopy*, Perkin-Elmer Corporation

[9]G.R. Sparrow and I.W. Drummond, "Surface Analysis: Selecting a Technique and an Instrument," *Industrial Research and Development*, 112-115, August 1981.

[10]D.T. Clark and H.R. Thomas, "Application of ESCA to Polymer Chemistry. XVI. Electron Mean Free Paths as a Function of Kinetic Energy in Polymeric Films Determined by Means of ESCA," *Journal of Polymer Science: Polymer Chemistry Edition*, **15**, 2843-2867 (1977)

[11]P.M.A. Sherwood, "Appendix 3: Data Analysis in X-ray Photoelectron Spectroscopy," *Practical Surface Analysis by Auger and X-ray Photoelectron Spectroscopy*, Edited by D. Briggs and M.P. Seah, John Wiley & Sons, (1983).

CHAPTER 3

POLYIMIDE CHEMISTRY, CHARACTERIZATION, and PROPERTIES

POLYIMIDE CHEMISTRY

Polyimide is a generic term for a large class of polymer molecules which are condensation products of a dianhydride and dianiline reaction. The monomers and resulting polyimide are shown in Figure 3-1. The imide linkage is the $(C=O)_2NC$ chemical structure in the polymer and was found to be stable up to approximately 500°C in nitrogen.[1] R and R' are aromatic or other heat-resistant groupings, which allow the polyimides' properties to be modified and controlled while utilizing the temperature resistance of the imide linkage. In this manner polyimides offer a totality of excellent physical and mechanical properties which are stable under prolonged thermal exposures.

The specific polyimide chosen for this work is the one produced from pyromellitic dianhydride (PMDA) and 4,4'-oxydianiline (ODA). The PMDA/ODA polyimide was selected because of its more widespread usage, relatively simpler chemical structure, and more extensive characterization in literature. PMDA/ODA polyimide is commercially available from the DuPont Company as Kapton film, which has been used for wire insulation[2], or as the polyamic acid precursor PI-2545. Figure 3-2 shows the PMDA and ODA monomers, as well as the PI-2545 polyamic acid and the resulting polyimide.

Figure 3-1. Polyimide Synthesis

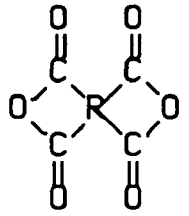

Dianhydride

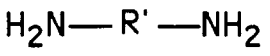

Diamine

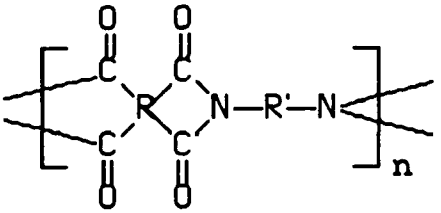

Polyimide

The PMDA/ODA polyamic acid is formed by adding the PMDA to a solution of ODA, in which a charge transfer condensation reaction occurs. A polar solvent, in this case N-Methyl-2-Pyrrolidone (NMP), is required to form the polyamic acid. The ability to spin- or spray-coat this solution with excellent uniformity across a wafer makes the polyimide excellent for passivation and planarization layers in the microelectronics industry.[3,4] The insoluable polyimide film is then formed by dehydration of the polyamic acid, usually by thermal means.

Several researchers have recently shown the PMDA/ODA polyamic acid can be deposited solventless by codeposition of PMDA/ODA using molecular beam epitaxy.[5,6,7] This technique may prove important where solvent effects are deleterious.

Figure 3-2. Chemistry of PMDA/ODA Polyimide

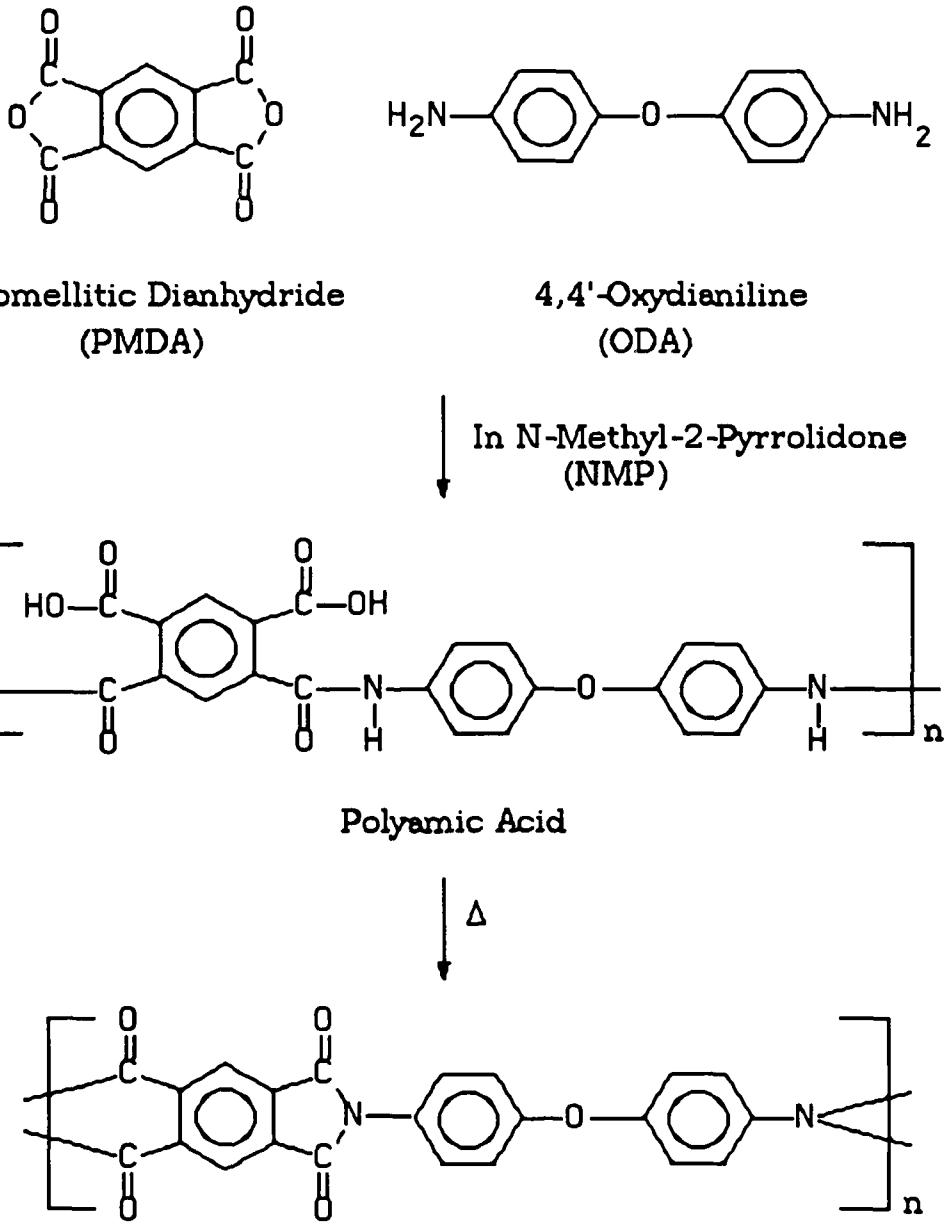

Figure 3-3. Monomers of PI-2555

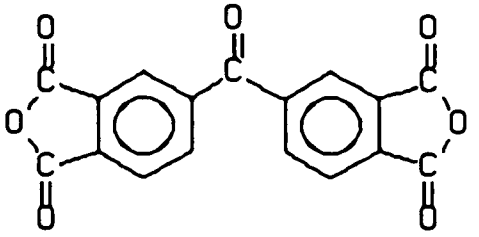

Benzophenone tetracarboxylic dianhydride
(BTDA)

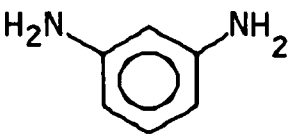

Meta-phenyldiamine
(MPD)

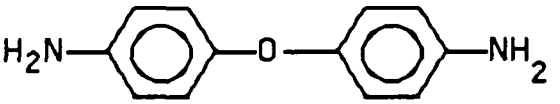

4,4'-Oxydianiline
(ODA)

The polyimide from benzophenone tetracarboxylic dianhydride (BTDA) and ODA was also considered for this work because published data suggests better strength, intercoat adhesion, and thermal stability due to crosslinking in addition to imidization during curing.[8] This polyimide is available commercially as PI-2555 , which has the additional m-phenylene diamine (MPD) monomer[9] as shown in Figure 3-3. The diamine monomers are present in approximately a 3 parts ODA : 2 parts MPD ratio. The resulting polyimide is a copolymer consisting of BTDA/ODA and BTDA/MPD blocks. Due to the more complex chemistry caused by two diamine monomers and an additional C=O functionality, the PI-2555 was not used in this study.

It should, however, be considered for subsequent polyimide/metal interface studies.

INFRARED SPECTROSCOPY CHARACTERIZATION

The infrared spectrum (IR) of PMDA/ODA polyimide was thoroughly characterized by Ishida *et al*[10], who used model molecules to assign specific chemical structures to a significant number of the IR absorption peaks. Figure 3-4 shows the IR transmission spectrum of cured PMDA/ODA polyimide from 2000-400 cm^{-1}, with peak assignments given in Table 3-1. This sample was prepared by spin-coating the PI-2545 onto a silicon wafer and curing at 250°C. The

Table 3-1. IR Absorption Peak Assignments for PMDA/ODA Polyimide

Peak Location (cm^{-1})	Assignment
1776	υ(C=O) in-phase
1724	υ(C=O) out-of-phase
1597	υ_{16} 1,4-C_6H_4
1501	υ_{13} 1,4-C_6H_4
1454	$\delta(CH_2)C_6H_{11}$
1377	$\upsilon(CN)(OC)_2NC$
1244	υ_{as}(COC)
1169 & 1115	Imide III $(OC)_2NC$
1015	υ_6 1,2,4,5-C_6H_2
918	υ_{11}' 1,2,4,5-C_6H_2
822	γ_w 1,2,4,5-C_6H_2
725	Imide IV
604	υ_{18} 1,4-C_6H_4
567	δ_{as}(C,C > NC)
1288, 1092, 881, 519, 429	Unidentified

Figure 3-4. IR Spectrum of Cured PMDA/ODA Polyimide

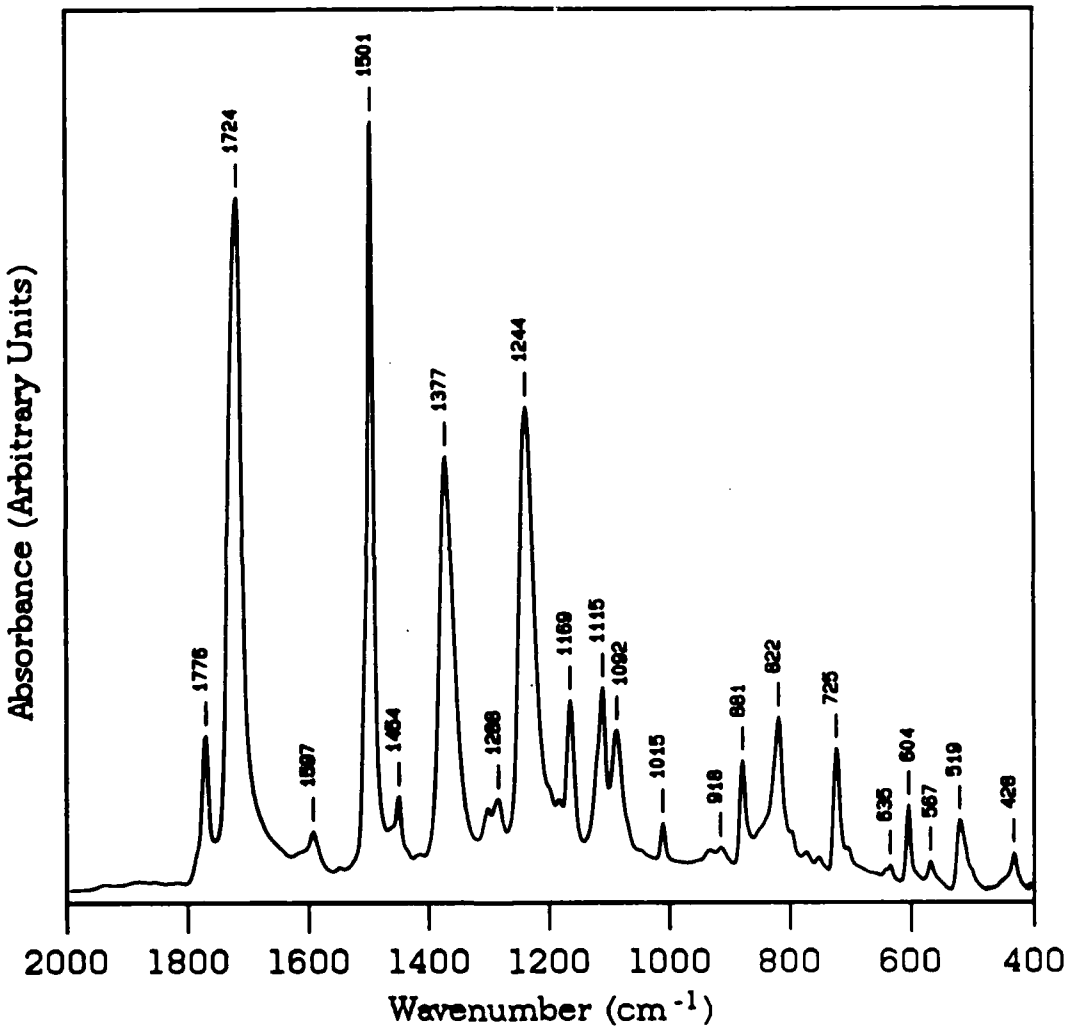

resulting 1.1 μm film was removed from the wafer after soaking the film in deionized water. The spectrum was collected using the IR instrument described in Chapter 5.

Another chemical structure, referred to as isoimide, is known to be present in polyimides.[11,12] This structure which has the same chemical composition as normal imide is shown in Figure 3-5. A strong, broad absorption peak around 915 cm^{-1} is typical for the PMDA/ODA isoimide.[12,13] The % isoimide is obtained by referencing the 915 cm^{-1} absorption to a characteristic imide peak, typically the one at 720 cm^{-1}. Buchwalter and Baise[14] and Chauvin *et al* [15] used IR

Figure 3-5. PMDA/ODA Isoimide

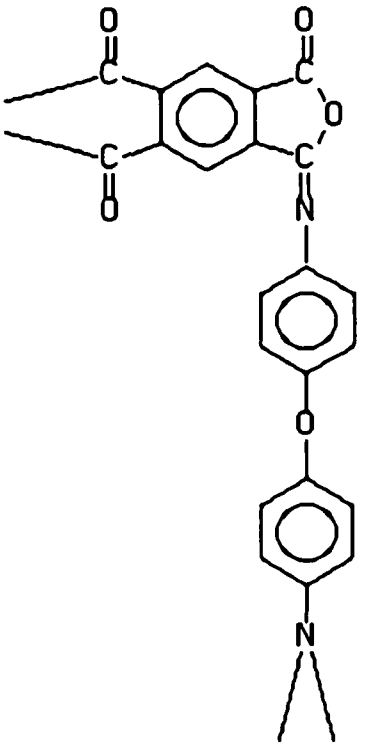

and other techniques to show that polyimide surfaces consist of 6.5-8% isoimide. Chauvin *et al* [15] used nuclear scattering techniques to verify that the composition of the polyimide films were independent of depth. The broad region around 918 cm^{-1} in Figure 3-4 may be due to a small percentage of isoimide at the surfaces of the thick PMDA/ODA film.

The imidization (curing) process can be followed by monitoring changes in the infrared spectrum. Figure 3-6 shows the IR spectra acquired on the PMDA/ODA polyimide for this thesis. During imidization the amide (N-H) and carboxylic acid (COOH) groups are converted to the cyclic imide (C-N) structure. The result is the weakening of the amide peaks around 3300 cm^{-1} and 1540 cm^{-1} and the development of imide peaks around 1380 cm^{-1} and 720 cm^{-1}. The C=O carboxylic acid character is lost around 1660 cm^{-1}, while a doublet with peaks near 1780/1725 cm^{-1} develops due to the cyclic C=O structure. Ishida *et al* [10] proposed the C=O doublet arose from symmetric and asymmetric vibrations of the C=O group. Frayer[16] has proposed that the 1725 cm-1 band is a mixed mode band whose intensity is enhanced by the addition of the second C=O group to the original N-(C=O) structure in the polyamic acid.

The rate of imidization determined from following the1780 cm^{-1} peak is higher than that determined by the 1380 cm^{-1} peak, apparently due to hydrogen bonding between carbonyl groups and unconverted carboxylic acid groups.[1] The 720 cm^{-1} peak follows the 1380 cm^{-1} peak during curing. For the PMDA/ODA polyimide, the

Figure 3-6a. IR Spectra of PI from 4000-400 cm^{-1} during Imidization

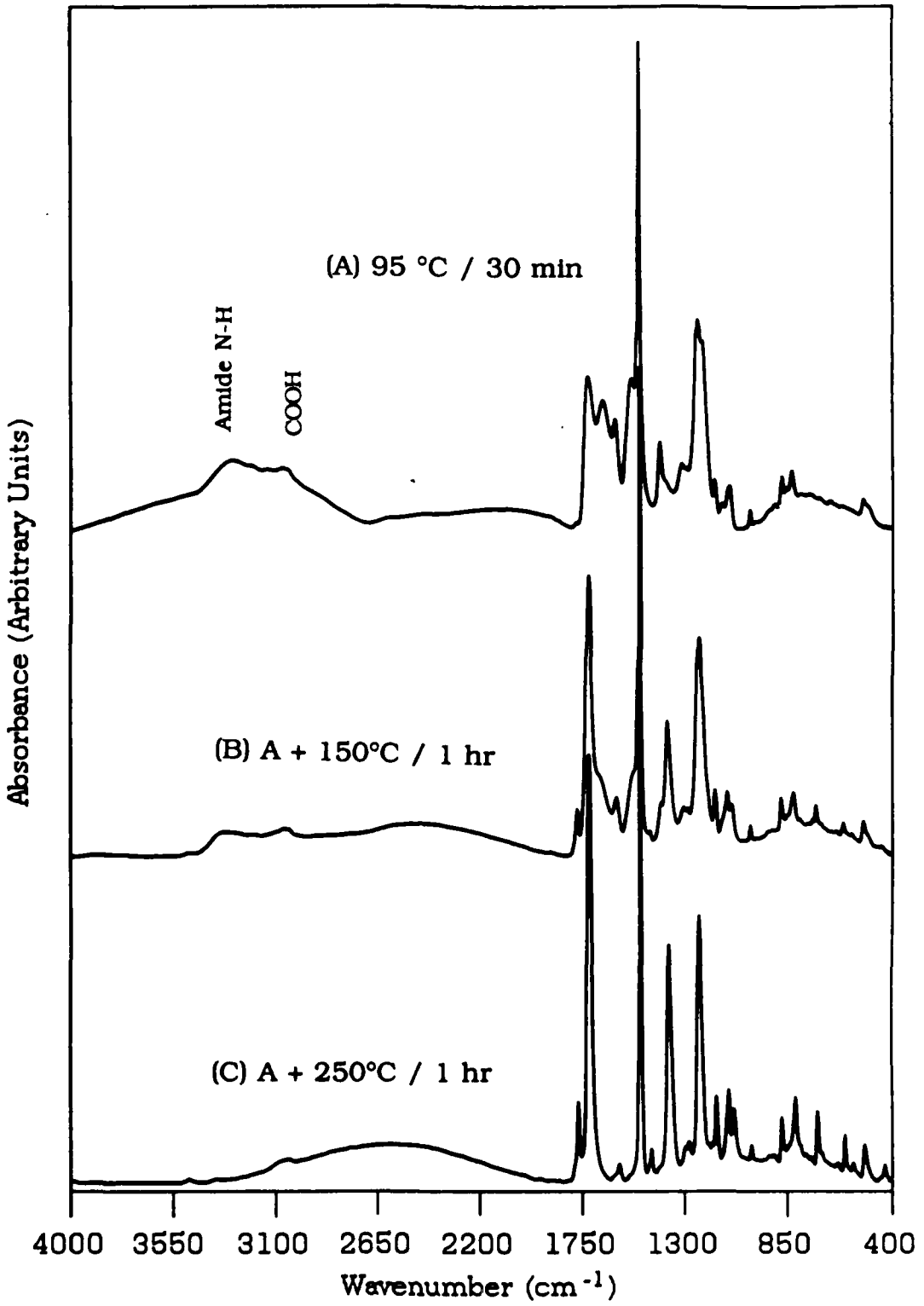

Figure 3-6b. IR Spectra of PI from 2000-400 cm^{-1} during Imidization

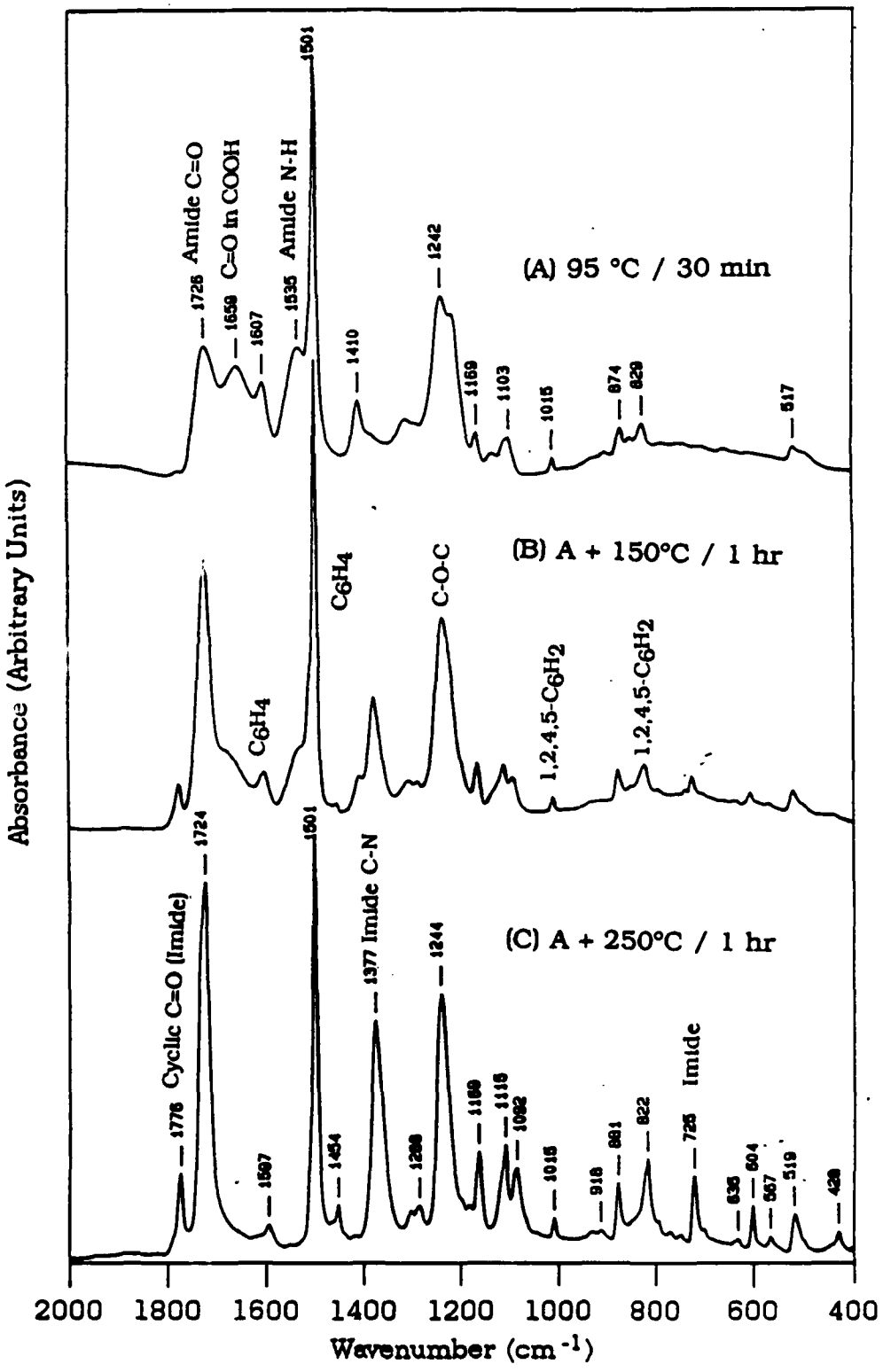

peaks' intensities stopped increasing after 15 minutes at 300°C, indicating completion of imidization.

The imidization rate constant follows Arrhenius' equation for a given imidization; however, the rate constant activation energy increases with increasing degree of imidization. This may be caused by decreased mobility of the polyimide as the number of imide rings formed increases. The imidization rate was shown to be a function of solvent content, with samples cured without prior heat treatment imidizing more rapidly than ones with a preliminary bake. It remains to be shown whether the solvent effect is merely plasticization or is directly participating in the imidization through chemical bonding to the polyamic acid.[1]

A debate remains over whether imidization is complete when no further changes are seen in the characteristic IR peaks. From the IR spectra, imidization is complete after about 15 minutes at 300°C. However, important properties of the polyimide change significantly after higher temperature exposures. For example, the elastic modulus of PMDA/ODA polyimide exhibits a fourfold decrease when the final temperature is raised from 200°C to 400°C.[1] Likewise, the dissipation factor at 1 MHZ decreases from 0.018 to 0.007 over the same temperature range.[17] Some theories suggest further imidization is occurring. Others suggest secondary chemical transformations occur which lead to the formation of inter-chain bonds (crosslinking).

X-RAY PHOTOELECTRON SPECTROSCOPY CHARACTERIZATION

The electron binding energy characteristics of the PMDA/ODA polyimide have been characterized by x-ray photoelectron spectroscopy (XPS) using model compounds to attribute specific chemical structures to binding energy peaks. The initial assignments based on empirical data[14,18] have been supported by more recent molecular orbital calculations.[19,20] Figure 3-7 shows the XPS C-1s, N-1s, and O-1s bands acquired for this research. A summary of published XPS band assignments for the PMDA/ODA polyimide is given in Table 3-2.

Table 3-2. XPS Analysis of PMDA/ODA Polyimide

Element & Orbit	Binding Energy (eV)	ΔBE (eV)	Assignment
Carbon-1s	285.0-285.3	0	Aromatic C's [14,18-21]
	286.1-286.3	1.0-1.1	Aromatic C-O & C-N [14,18-21] + PMDA C's [14,19-21]
	288.8-289.3	3.8-4.0	C=O [14,18-21]
	292.0		$\pi-\pi^*$ [14]
Nitrogen-1s	399.3	(1.5-1.7)	Isoimide N [14]
	400.5-401.0	0	Imide N [14,18,21]
Oxygen-1s	532.1-532.5	0	C=O [14,18,21]
	533.7-533.8	1.2-1.7	C-O-C [14,18,21]

Figure 3-7. XPS Spectra for Cured PMDA/ODA Polyimide

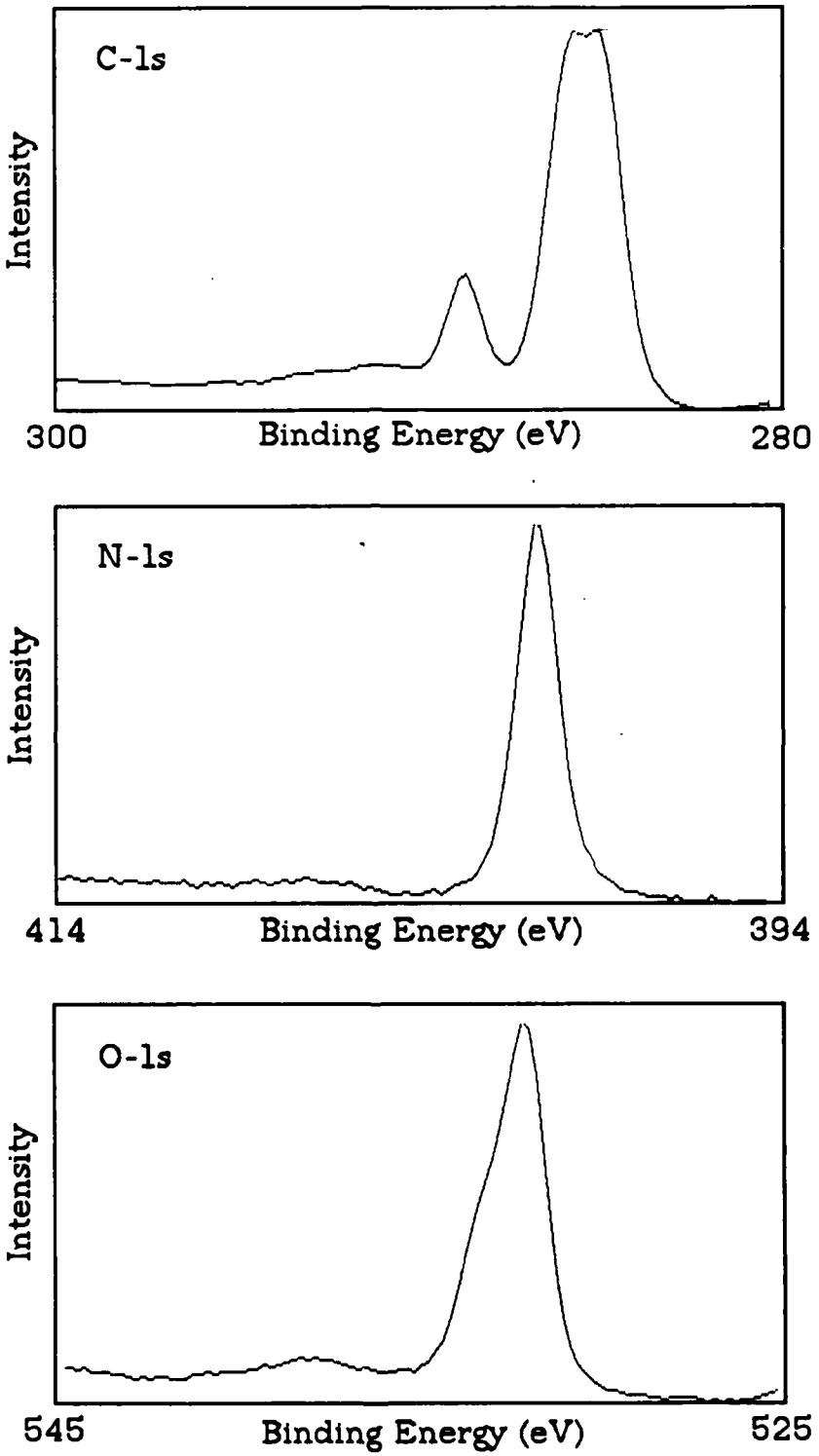

Polyimide has a C-1s spectra which actually consists of three peaks, as determined by curve-synthesis analysis. The low binding energy peak is from aromatic carbon; the middle peak is from aromatic carbon with single bonds to nitrogen or oxygen and the aromatic carbons in the PMDA ring, and the high binding energy peak is due to carbonyl carbon. Theoretically four of the twenty-two carbon atoms in the PMDA/ODA repeat unit would have carbonyl character. Experimental data, however, has shown the polyimide to be carbonyl deficient.[18,21] The deficiencies range from 2.9 to 3.3 carbonyl carbons per repeat unit.

The PMDA carbons are shifted from the aromatic carbon component at 285.0 eV to the 286.1 eV component due to the electron withdrawing character of the carbonyl group.[14] Buchwalter and Baise empirically found three carbonyl groups were required to achieve this shift. Molecular orbital calculations have supported this finding, showing that carbonyl groups induce shifts in the C-1s binding energies, with the amount of the shift depending on the number of carbonyl groups attached to the aromatic ring. For a structure like PMDA, with four attached carbonyl groups, a shift of about 1 eV is predicted. As a result the C-1s spectrum for the PMDA carbons is superimposed on the peak due to C-N/C-O environments.

The O-1s spectra can be separated into contributions from two different oxygen states: carbonyl oxygen and ether oxygen. Data from the O-1s region has supported the carbonyl deficiency found in the C-1s band. Leary and Campbell[18] found a C=O/C-O-C ratio of 2.7, while Anderson *et al*[21] reported a 2.3 ratio versus the theoretical value of

four. In Leary and Campbell's work the surfaces approached, but never reached, the expected C=0/C-O-C ratio as cure temperature increased. The deficiency was apparently caused by rearrangement within the polymer since overall analysis of the film showed the film to have the correct proportions of carbon, oxygen, and nitrogen.[21]

Leary and Campbell[18] also reported a second N-1s component at 289.0 eV, which comprised 2 to 8.5% of total N signal for all cured polyimide surfaces. The percentage was a function of polyimide type and cure conditions. Their observations fit the trends expected from the isoimide structure of Figure 3-5, which yields a second nitrogen electronic state and reduces the carbonyl groups on the surface of the polyimide. Anderson *et al* [21] did not observe the low energy component in completely cured films, possibly because of a higher cure temperature for the reported data. They did, however, find lower binding energy components when the film was degraded above 450°C.

In their work, XPS was used to study the curing and degradation of PMDA/ODA polyimide as a function of time and temperature. The studies were conducted with 180 Å films on aluminum-coated silicon wafers. During the dynamic curing, significant changes occurred in the C-1s, N-1s, and O-1s bands between 200 and 300°C Carbon and nitrogen intensities increased, while oxygen intensity decreased. These trends correspond to the loss of water during imidization as shown in Figure 3-2. From 300 to 450°C no compositional changes were observed.

Between 450 and 500°C, however, rapid changes occurred in the XPS bands. Significant losses were observed in the oxygen and nitrogen content of the films, while the carbon content increased slightly. The increase was attributed to proportionally more oxygen and nitrogen leaving in degradation products like CO_2, CO, N_2, H_2, and H_2O.

The C-1s and O-1s bands indicated that the carbonyl group was most effected during the degradation process. During degradation the N-1s band exhibited components approximately 1.3 and 1.7 eV below the primary imide component. The component 1.3 eV lower emerged first and was attributed to nitrogen double-bonded to carbon or to hydrogenated nitrogen. The component 1.7 eV lower emerged after extended time at 500°C and was attributed to triple-bonded nitrogen species.

REFERENCES

[1]N.A. Adrova, M.I. Bessonov, L.A. Laius, and A.P. Rudakov, *Polyimides: A New Class of Heat-Resistant Polymers*, Translated from Russian by J. Schmorak, Israel Program for Scientific Translations (1969).

[2]J.F. Heacock, "A Kinetic Study of the Hydrolysis of Polyimide Film," *Recent Advances in Polyimide Science and Technology*, Edited by W.D. Weber and M.R. Gupta, 174-190, The Mid-Hudson Chapter of The Society of Plastics Engineers, Inc. (1987).

[3]A.M. Wilson, "Use of Polyimides in VLSI Fabrication," *Polyimides: Synthesis, Characterization, and Applications*, Edited by K.L. Mittal, 715-733, Plenum Press (1984).

[4]D.R. Day, D. Ridley, J. Mario, and S.D. Senturia, "Polyimide Planarization in Integrated Circuits," *Polyimides: Synthesis, Characterization, and Applications*, Edited by K.L. Mittal, 767-781, Plenum Press (1984).

[5]J.R. Salem, F.O. Sequeda, J. Duran, W.Y. Lee, and R.M. Yang, "Solventless Polyimide Films by Vapor Deposition," *J. Vac. Sci. Technol.*, **A4 (3)**, 369-374 (1986).

REFERENCES (continued)

[6]M. Grunze and R.N. Lamb, "Summary Abstract: Characterization of Ultrathin Polyimide Films (d=11 Å) Formed by Vapor Deposition of 4,4-Oxydianiline and 1,2,4,5-Benzenetetracarboxylic Anhydride," *J. Vac. Sci. Technol.*, **A5 (4)** , 1685-1686 (1987).

[7]S.P. Kowalczyk, Y.H. Kin, G.F. Walker, and J. Kim, "Polyimide on Copper: The Role of Solvent in the Formation of Copper Precipitates," *Appl. Phys. Lett.*, **52 (5)**, 375 - 376(1988).

[8]DuPont Pyralin Polyimide Coatings for Electronics, PI-2550, PI-2555, PI-2540, PI-2545 Semiconductor Grade, Bulletin #PC-1 (E-20947), DuPont Company, Wilmington, DE.

[9]W.D. Weber and M.R. Gupta, "Molecular Weight/Property Relationships in a Series of Polyimide Copolymers," *Recent Advances in Polyimide Science and Technology*, Edited by W.D. Weber and M.R. Gupta, 214-224, The Mid-Hudson Chapter of The Society of Plastics Engineers, Inc. (1987).

[10]H. Ishida, S.T. Wellinghoff, E. Baer, and J.L. Koenig, "Spectroscopic Studies of Poly[N,N'-bis(phenoxyphenyl)pyromellitimide]. 1. Structures of the Polyimide and Three Model Compounds," *Macromolecules*, **13**, 826 -834(1980).

[11]R.A. Dine-Hart and W.W. Wright, "Preparation and Fabrication of Aromatic Polyimides," *J. Appl. Polym Sci.*, **11**, 609-627 (1967).

[12]F.P. Gay and C.E. Berr, "Polypyromellitimides: Details of Pyrolysis," *J. Polym. Sci., A-1* , **6**, 1935-1943 (1968).

[13] R.J. Angelo, R.C. Golike, W.E. Tatum, and J.A. Kreuz, "Cyclization Studies of Amic Acids to Imides and Isoimides: Monomeric and Polymeric Reactions," *Recent Advances in Polyimide Science and Technology*, Edited by W.D. Weber and M.R. Gupta, 67-91, The Mid-Hudson Chapter of The Society of Plastics Engineers, Inc. (1987).

[14]P.L. Buchwalter and A.I. Baise, "ESCA Analysis of PMDA-ODA Polyimide," *Polyimides: Synthesis, Characterization, and Applications*, Edited by K.L. Mittal, 537-545, Plenum Press (1984).

[15]C. Chauvin, E. Sacher, and A. Yelon, "The Density and Composition of Polyimide Surface Layers," *J. Appl. Polym. Sci.*, **31**, 583 -587 (1986).

[16]P.D. Frayer, "The Interplay Between Solvent Loss and Thermal Cyclization in LARC-TPI," *Polyimides: Synthesis, Characterization, and Applications*, Edited by K.L. Mittal, 273-294, Plenum Press (1984).

[17]G. Samuelson, "Polyimide for Multilevel Very Large-Scale Integration," *Polymer Materials for Electronic Applications*, edited by E.D. Feit and C.W. Wilkins, Jr., ACS Symposium Series 184, American Chemical Society, 93-106 (1982).

REFERENCES (continued)

[18] H.J. Leary and D.S. Campbell, "Surface Analysis of Aromatic Polyimide Films Using ESCA," *Surface and Interface Analysis*, **1 (3)**, 75 -81 (1979).

[19] B.D. Silverman, P.N. Sanda, P.S. Ho, "Origin of the Carbon 1s-Core Level Shifts in Polyimide Model Compounds," *J. Polym. Sci.: Polymer Chemistry Edition*, **23**, 2857-2863 (1985).

[20] B.D. Silverman, P.N. Sanda, J.W. Bartha, P.S. Ho, and A.R. Rossi "Molecular Orbital Analysis of the XPS Spectra of Polyimide Model Compounds," *Recent Advances in Polyimide Science and Technology*, Edited by W.D. Weber and M.R. Gupta, 233-239, The Mid-Hudson Chapter of The Society of Plastics Engineers, Inc. (1987).

[21] S.G. Anderson, H.M. Meyer, III, Lj. Atanasoska, and J.H. Weaver, "Dynamics of Polyimide Curing and Degradation: An *in situ* X-ray Photoemission Study," *J. Vac. Sci. Technol.*, **A6(1)**, 38-43 (1988).

CHAPTER 4

BACKGROUND INFORMATION ON POLYIMIDE / METAL INTERFACES

INTRODUCTION

Several studies have used a variety of surface spectroscopy techniques to elucidate the nature of metal-polymer interactions. The most widely used surface probes have been x-ray photoelectron spectroscopy (XPS) and UV photoemission spectroscopy (UPS), which were used to analyze successive monolayer depositions of metal on cured polyimide. In addition, results from Auger analysis (AES), high resolution medium energy ion scattering (MEIS), and electron energy loss spectroscopy (EELS) were correlated with the XPS and UPS results. Transmission electron microscopy (TEM) was used by a few researchers to study the interfacial morphology and to confirm theories on processes occurring at the interfaces. Limited data is available on the study of these interfaces by infrared techniques.

Chou and Tang[1] have presented thermodynamic arguments which suggest that metals with large heats of sublimation and heats of oxide formation will react with polyimide by breaking the carbonyl bonds. The calculations predict metals like aluminum, chromium, nickel, and titanium will react with polyimide, while metals like copper, gold, and silver will not. In this paper , Chou and Tang presented XPS data which indicated chromium and nickel were reactive and copper and silver were not. The following discussion summarizes the results of studies on the reactive nature of

metal/polyimide systems of interest to the microelectronics community.

COPPER-POLYIMIDE INTERFACE

Copper on Polyimide

The interface formed when successive monolayers of copper were deposited *in situ* onto imidized polyimide has been extensively studied by XPS experiments. While Chou and Tang[1] observed a proportional decrease in the resolved C-1s polyimide peaks, Hahn *et al.*[2] and Ho *et al.*[3] found the peak associated with the C-1s carbonyl bonds decreased faster than the other C-1s peaks, suggesting some interaction of the copper with the polyimide through the C=O structures, but not enough to alter the chemical nature of the surface. These studies were conducted by depositing the copper at room temperature. With these room temperature copper depositions, annealing at 300°C recovered a significant portion of the original polyimide character in the XPS spectrum.[3] The data for the Cu-2p peak indicated copper remained in the metallic state throughout deposition .[1,2]

UPS studies[2,3] indicated the same behavior. With room temperature depositions, polyimide features were depressed, while the 3d valence structure of unreacted, metallic copper developed. Upon annealing, the intensity of the 3d peak dropped, and the polyimide characteristics recovered. The recovery of XPS and UPS polyimide characteristics upon annealing could be explained by cluster formation and/or intermixing. The XPS and UPS results are consistent with

cluster formation since analyses indicated metallic copper throughout the deposition process.

MEIS analysis,[4] a mass and depth dispersive technique, showed that copper deposited at room temperature does not form uniform films and has a depth distribution that does not change with increasing coverage. The spectra never reached that expected for a continuous, pure copper film. After the 300°C anneal, MEIS found the copper was covered by a 5 Å overlayer. Samples with copper deposited at successively higher temperatures indicated that the copper diffused deeper into the polyimide matrix as the deposition temperature increased, with the MEIS spectra having a maximum below the surface. TEM micrographs[4] showed the copper in the intermixed region forms spherical clusters which are uniform in size at a given deposition temperature, but increase in size with increasing deposition temperature.

These results indicate the processes occurring at the copper-polyimide interface during copper deposition onto polyimide to be predominantly physical in character, with copper clustering and intermixing with the polyimide. The extent of intermixing and cluster size are a strong function of temperature, with both increasing with temperature.

Polyimide on Copper

Fewer studies have considered the processes which occur when polyimide is deposited onto metal. The chemical and physical differences between polyamic acid/metal versus metal/polyimide

interactions are critical since typical fabrication processes require deposition and curing on metal films. Associated process issues are solvent and thermal effects.

Kelley *et al* [5] considered the interaction of polyimide and copper at elevated temperatures using reflection-absorption (RA) and attenuated total reflection (ATR) spectroscopy. During curing for successively longer times at 250°C in air, the imide ring absorption bands and the aromatic C-H in-plane bending absorption band at 1114 cm^{-1} were reduced. A new band attributed to nitrile groups appeared at 2186 cm^{-1}, and multiple bands attributed to oxidized products appeared in the 1600-1500 cm^{-1} region. Kelley *et al* concluded that copper-catalyzed degradation of polyamic acid was competing with imidization during the cure process. Carboxylate salts and nitriles were identified as two of the degradation products. Studies with curing in air and nitrogen indicated oxygen plays a role in the degradation process.

In another study considering the polyimide-on-copper structure, Kowalczyk *et al* [6] prepared solventless PMDA/ODA polyamic acid on copper foil (with native oxide) using molecular beam deposition. One sample was treated with NMP to simulate the more common spin-coated films. The cured films were around 7500 Å thick.

When the solventless films were imidized, a sharp polyimide/copper interface was formed. However, imidization with NMP present resulted in the formation of copper precipitates in the polyimide film, with a 500 Å polyimide zone near the interface free of the precipitates. Apparently the polyamic acid reacted with the

copper oxide surface, forming carboxylate which decomposed during curing. The solvent provided mobility to the precipitates, allowing them to diffuse and aggregate.

These studies verified that polyimide/metal interfaces are not inert. Because of the growth sequence dependence and solvent effects, the interfacial and bulk properties of polyimide insulators may be significantly different.

GOLD-POLYIMIDE INTERFACE

Meyer *et al* [7] studied the deposition of gold onto PMDA/ODA polyimide by XPS. They found no evidence for chemical interactions of gold and polyimide. While the resolved C-1s polyimide peaks decreased proportionally, the attenuation rate of polyimide(C-1s, N-1s, and O-1s) signal was significantly different from that of a metal film completely covering of the substrate. In addition, although a uniform shift of all substrate spectra to lower binding energies occurred with increasing gold coverage, the relative positions of the C-1s and O-1s components were unchanged. The overall spectra shift was attributed to photon-induced injection of charge into the polyimide.

The nonlinear growth of the Au $4f_{7/2}$ emission versus coverage confirmed the the formation of a heterogeneous gold overlayer. The shift of the Au $4f_{7/2}$ to lower apparent binding energy with increasing coverage matched results of previous studies on the effects of gold cluster size on XPS spectra.

The above results indicated gold grew on the polyimide surface through nucleation and growth of gold islands, with no chemical interactions between the gold and polyimide.

ALUMINUM-POLYIMIDE INTERFACE

Several studies have looked at the process which occurs during aluminum deposition onto cured polyimide during. *In situ* XPS analysis for depositions made at 300°C showed the C-1s carbonyl peak decreased more rapidly with increasing metal coverage than the other polyimide C-1s contributions and two new C-1s peaks appeared. One new C-1s peak, which appeared approximately 1.7 eV below carbonyl at low metal coverages, was attributed to a shift in the carbonyl peak through moderate chemical interactions between aluminum and the carbonyl groups. The second new C-1s peak, which appeared at high aluminum coverages, occurred at lower binding energies in a region typical for aluminum carbides. [3,8]

The polyimide N-1s peak showed a weak decrease in intensity, with a new, lower binding energy peak appearing at high coverages.[3,8] The region of the new contribution is indicative of aluminum nitrides. Decreases in the carbonyl contribution to the O-1s peak were also observed with increasing aluminum coverage.

At low coverages the Al-2p peak showed strong oxide character but shifted to a peak typical of metallic, unreacted aluminum at higher coverages. Unreacted aluminum was not seen in initial deposits. When the metallic character emerged, it was shifted roughly 1.5 eV higher than the standard metallic Al-2p peak. This shift correlated with the

C-1s shift, although no change was observed in the O-1s state. The amount of the Al-2p shift did not support the formation of Al_2O_3, suggesting the formation of Al-O-C complexes. At intermediate coverages, a broad peak containing characteristics of both aluminum states was seen. A significant observation by Bartha *et al.* was that the increase in aluminum intensity and decrease in polyimide characteristics were less than that expected for a homogeneous aluminum layer,[1,7] suggesting growth involving intermixing and/or island formation.

Subsequent XPS work by Atanasoska *et al*[9] using room temperature depositions of aluminum onto polyimide produced supporting data. These experiments sampled more data points for coverages below 1 Å, giving greater insight into the initial phases of the reaction process.

Initially, the N-1s signal attenuated more rapidly than either the C-1s or the O-1s, indicating the aluminum preferred the planar imide ring. Eventually the decay rates of the polyimide's characteristic signals became equal; however, their decay rate and the growth rate of the Al-2p emission were less than that predicted for growth of a uniform, layer-by-layer film.

The decomposed C-1s spectra showed enhanced carbonyl decay relative to the overall C-1s decay and to the decay of the other carbonyl contributions. Thus, as with the 300°C deposits, the aluminum reacted with the polyimide at the carbonyl groups. A finding which correlated with previous observations on chromium depositions (see below) was a relatively slower decay of the C-1s contribution from the aromatic C-C

structures. Apparently, as suggested by Jordan *et al* [12] for the chromium reaction, the aluminum interaction with the carbonyl groups causes a relaxation of charge withdrawal from the PMDA aromatic ring. As a result the PMDA ring recovers its benzene ring nature, shifting its contribution to the C-1s spectra to lower binding energies. The decomposed C-1s spectra also showed a reaction-induced peak near the C-O region (~ 1.6 eV below carbonyl) for the initial stages of deposition. This also follows the pattern observed for chromium and for high temperature aluminum depositions, although in the case of chromium the C-1s signal was not decomposed into the four contributions. Similar analysis of the O-1s peak showed initial growth of the ether region, with equal attenuation of both the ether and carbonyl contributions at higher coverages. The C-1s and O-1s trends indicated initial reaction with the carbonyl groups, inducing an ether-like oxidation state, at low coverages. At higher coverages, the first reaction-induced peak gives way to one at lower binding energies, indicating the carbonyl carbon atoms are carrying an excess negative charge in the C-O-Al complex.

The growth profiles for contributions to the Al-2p peak showed oxidized aluminum dominated at low coverages, reached a maximum, and then attenuated. Metallic aluminum contribution was initially small, but grew exponentially to dominate at higher coverages. The observed shift of the oxide shoulder relative to metallic aluminum was around 1.7 eV, which corresponded with results of the 300°C depositions.

Annealing of the structures at 300°C produced no recovery of the polyimide XPS character as was the case for copper, but further developed the reaction induced feature and produced an even lower binding energy peak, apparently due to carbide formation. The N-1s spectrum, which had only a single feature upon deposition, was composed of three features after annealing: n-imide, cleaved imide bonds, and aluminum nitride. The appearance of the carbide and nitride species had been observed for the higher temperature depositions.

UPS studies[3] on aluminum deposited at room temperature showed depression of the polyimide characteristics with increasing coverage. Slight recovery of the polyimide characteristics occurred upon 300°C annealing. The weak intensity of the XPS Al-2p peak and the recovery of polyimide characteristics in the UPS spectra upon annealing were explained by intermixing and/or cluster formation. However, the lack of unreacted aluminum character in initial deposits indicated clustering did not occur. TEM micrographs of high coverages deposited at 300°C confirmed the small intermixed region and the growth of aluminum islands.[1,7] No separate Al_2O_3 phase could be identified. Thus, the TEM micrographs confirmed the XPS results.

The lack of an Al_2O_3 phase and the Al-2p and C-1s carbonyl peak shifts indicate the aluminum initially interacts with the polyimide at the carbonyl groups, forming Al-O-C complexes. The initial enhanced N-1s decrease indicates aluminum nucleates on the planar imide ring, while the rate of attenuation of polyimide character indicates the growth of islands which grow more rapidly thicker than laterally. The

low binding energy C-1s and N-1s peaks at high coverages are most likely the result of a second electron transfer in which carbides and nitrides are formed in the metal-oxygen-polyimide complex. As the result of the chemical interaction, limited aluminum-polyimide intermixing occurs, without cluster formation. The amount of intermixing is dependent upon the deposition temperature. Thus, contrary to the case for copper and gold, aluminum forms chemical bonds with the polyimide.

CHROMIUM-POLYIMIDE INTERFACE

Chromium on Polyimide

The chromium/polyimide interface has been the focus of much attention due to its strength, up to six times greater than the copper/polyimide interface.[1] Peel tests results[10] confirm that the bond between polyimide and chromium is indeed a strong chemical bond. The chromium-polyimide bonds tested in this study showed strong initial strength, with no adhesion degradation upon aging at room temperature for 2 months or at 85°C/80% relative humidity for 16 hours. These characteristics have resulted in the use of chromium as an adhesion layer between a copper conductor and polyimide insulators.[10]

For chromium deposits on polyimide, the XPS spectra[1,2,11,12] showed a very rapid decrease at low coverages in the C-1s carbonyl peak relative to the other C-1s contributions. Chou *et al* [11] also noted the middle C-1s peak increased slightly during the rapid carbonyl decrease, indicating possible conversion of C=O to C-O. The main peak

shifted to a higher binding energy and changed shape,[1,11] The rapid decrease in the XPS carbonyl peaks upon chromium deposition indicated chromium initially reacted strongly through the carbonyl group. At high chromium coverages, the change in the C-1s peak was consistent with the formation of carbides, which provide a lower binding energy contribution to the C-1s peak. Ohuchi and Freilich[15] were the first to identify carbides as a product of metal/polyimide reaction based on XPS and Auger spectroscopic studies of the titanium/polyimide interface.

Significant changes were also observed for the polyimide N-1s and O-1s spectra, including the shift of the N-1s peak to a lower binding energy at high coverages.[2] This trend was consistent with nitride formation.

The initial Cr-2p peak was typical of that found for the oxide doublet, while a trend toward metallic chromium emerged at higher coverages.[1,10] Thus, the first few monolayers of chromium were oxidized either by the formation of Cr-O complexes followed by scission of C-N bonds or by the formation of CrO, CrO_2, and Cr_2O_3 with the breakage of C=O bonds.

Annealed chromium/polyimide structures showed no recovery of the polyimide XPS character.[2]

XPS studies with model compounds confirmed the reaction location of the chromium. P.N. Sanda *et al* [13] used N,N'-diphenylpyromellitimide as the PMDA model and poly(2,6-dimethylphenylene oxide) as the ODA model. Jordan *et al* [12] used

poly(vinyl methyl ketone) for the PMDA model and the same ODA model as above.

Deposition of chromium on the polyimide and the PMDA models resulted in abrupt decreases in the carbonyl contribution to the C-1s spectra.[12,13] During initial chromium depositions *onto* the PMDA model, Jordan and co-workers[12] observed a C-1s increase in a region attributed to C-O type bonding, at a rate close to that of the carbonyl decrease, which indicated a change from C=O to C-O character. They also observed increases in the two lower binding energy C-1s contributions of the polyimide, with the increase in the aromatic C-1s contribution being very dramatic. Peaks typical of carbides developed with high chromium coverages for both the PMDA model and the polyimide.

Depositions on the ODA model showed a slight preference of the chromium for the ether linkages. A carbide peak again developed at high coverages.

The model studies again demonstrated that during deposition, chromium reacted with the carbonyl groups and did not drastically affect the ether linkages. As a result, the observed increase in the aromatic C-C contribution to the C-1s spectra was attributed to disruption of the electron-withdrawing character of the carbonyl groups due to interaction with the chromium, which allowed the PMDA ring to recover binding energies more typical of the benzene ring.

UPS spectra[2,14] for room temperature chromium deposition showed the strongest depression of polyimide character for the *in situ* UPS experiments. The UPS spectra initially showed no metallic

behavior, indicating complete oxidation of the chromium deposit. At high coverages the spectra indicated a uniform, metallic chromium layer. The spectra did not recover polyimide character after 300°C annealing. Thus, unlike aluminum and copper depositions, the UPS data for chromium indicated no intermixing of the metal and polyimide.

EELS was applied to characterize the behavior of near-surface polyimide vibrational modes upon chromium deposition.[13] With chromium depositions, a rapid downshift in the carbonyl C=O vibration was observed. This downshift indicates a reduction of C=O bond order by charge transfer from chromium into the carbonyl antibonding state, without the breaking of the original bond. With further depositions, the downshifted peak showed a relative intensity enhancement in the EELS spectra. This behavior contrasted that of palladium for which the EELS spectra showed a gradual, uniform attenuation of the polyimide vibrational bonds.

EELS results for chromium deposition also show the chemical bonding process to occur in two steps, the first being strong and rapid initial interaction by charge transfer from chromium to carbonyl to form Cr-O-C complexes. Dinardo suggested the second step is further reduction of the CO bond, resulting in breaking the original bond. This explanation, however, does not account for the evidence of carbide and nitride bonds.

TEM analysis [2,11] showed chromium deposits formed a flat, sharp interface, confirming no intermixing of the chromium and

polyimide. Despite strong oxide character in the XPS and UPS spectra, a distinct Cr_2O_3 phase could not be identified.

This reaction mechanism also supports the data from solution studies indicating no scissions in the polyimide backbone.

As with aluminum, a reasonable explanation which accounts for all the above evidence is the formation of complexes, in which a second electron transfer occurs. Chromium reacts almost immediately upon contact with the polyimide to form strong bonds, even at room temperature. The chemical reactions with the polyimide occur through initial electron transfer to the carbonyl group followed by a second electron transfer at higher coverages. The strong, rapid reactions prevent diffusion of the metals into the polymer matrix, resulting in sharp interfaces.

Polyimide on Chromium

Kelley *et al* [5] also considered the effect of chromium on the molecular structure of polyamic acid because of the widespread application of chromium as an adhesion layer in microelectronic applications. Using RA spectroscopy on polyimide/chromium structures, they did not observe the degradation of polyamic acid during curing as was found for polyimide on copper substrates. They attributed this difference to the formation of a stable oxide at the polyimide/chromium interface, which was identified as absorption peaks at 645 and 606 cm^{-1}. They suggest the tight oxide layer prevents the diffusion of chromium ions into the polymer, thus preventing chromium from catalyzing the reaction.

TITANIUM-POLYIMIDE INTERFACE

XPS data[15] showed the titanium reaction with polyimide to behave like that of chromium: rapid initial reaction of titanium with the polyimide carbonyl groups. The rapid decrease in the carbonyl XPS peak was accompanied by a shift in the Ti-2p from initial oxide nature to metallic nature. At high coverages peaks typical of carbide (Ti-C) bonds were seen.

UPS analysis showed an initial charge transfer from the Ti-3d state to the bond state with oxygen, with development of the Ti-3d state (more metallic in character) at higher coverages.

AES was used to show that the titanium deposit grew by the Stanski-Krautanar mode: formation of a complete first monolayer followed by development of islands. The AES spectra taken sequentially with XPS on identical titanium surfaces also showed the bonding changes at high coverages, which caused the new, low binding energy XPS C-1s peak, to have Ti-C characteristics.

REFERENCES

[1]N.J. Chou and C.H. Tang, "Interfacial Reaction During Metallization of Cured Polyimide: An XPS Study," *J. Vac. Sci. Technol.* , **A2 (2)**, 751-755 (1984).

[2]P.O. Hahn, G.W. Rubloff, J.W. Bartha, F.K. LeGoues, R. Tromp, and P.S. Ho, "Chemical Interactions at Metal-Polyimide Interfaces," Mater. Res. Soc. Symp. Proc. **40**, 251 (1985).

[3]P.S. Ho, P.O. Hahn, J.W. Bartha, G.W. Rubloff, F.K. LeGoues, and B.D. Silverman, "Chemical Bonding and Reaction At Metal/Polymer Interfaces," *J. Vac. Sci. Technol.*, **A3 (3)**, 739-745 (1985).

[4]R.M. Tromp, F.LeGoues, and P.S. Ho, "Interdiffusion at the Polyimide-Cu Interface," *J. Vac. Sci. Technol.*, **A3 (3)**, 782-785 (1985).

REFERENCES (continued)

[5]K. Kelley, Y. Ishino, and H. Ishida, "Fourier Transform IR Reflection Techniques For Characterization of Polyimide Films on Copper Substrates," *Thin Solid Films*, **154**, 271-279 (1987).

[6]S.P. Kowalczyk, Y.H. Kim, G.F. Walker, and J. Kim, "Polyimide on Copper: The Role of Solvent in the Formation of Copper Precipitates," *Appl. Phys. Lett.*, **52 (5)**, 375-376 (1988).

[7]H.M. Meyer,III, S.G. Anderson, L.J. Atanasoska, and J.H. Weaver, "X-ray Photoemission Investigations of Clustering and Electron Emission, Injection, and Trapping at the Gold/Polyimide Interface," *J. Vac. Sci. Technol.*, **A6 (1)** , 30-37 (1988).

[8]J.W. Bartha, P.O. Hahn, F.K. LeGoues, and P.S. Ho, "Photoemission Spectroscopy Study of Aluminum-Polyimide Interface," *J. Vac. Sci. Technol.*, **A3 (3)**, 1390-1393 (1985).

[9]L.J. Atanasoska, S.G. Anderson, H.M. Meyer, III, Z. Lin, and J.H. Weaver, "Aluminum/Polyimide Interface Formation: An X-ray Photoelectron Spectroscopy Study of Selective Chemical Bonding," *J. Vac. Sci. Technol.*, **A5 (6)** , 3325-3333 (1987).

[10]R.J. Jensen, J.P. Cummings, and H. Vora, Copper/Polyimide Materials System for High Performance Packaging," *IEEE Transactions on Components, Hybrids, and Manufacturing Technology*, **CHMT-7 (4)**, 384-393, December 1984.

[11] N.J. Chou, D.W. Dong, J. Kim, and A.C. Liu, "An XPS and TEM Study of Intrinsic Adhesion Between Polyimide and Cr Films," *J. Electrochem. Soc. : Solid-State Science and Technology*, **131 (10)**, 2335-2340 (1984)

[12]J.L. Jordan, P.N. Sanda, J.F. Morar, C.A. Kovac, F.J. Himpsel, and R.A. Pollak, "Synchrotron-radiation Excited Carbon 1s Photoemission Study of Cr/Organic Polymer Interfaces," *J. Vac. Sci. Technol.*, **A4 (3)**, 1046-1048 (1986).

[13]P.N. Sanda, J.W. Bartha, J.G. Clabes, J.L. Jordan, C. Feger, B.D. Silverman, and P.S. Ho, "Interaction of Metals with Model Polymers Surfaces: Core Level Photoemission Studies," *J. Vac. Sci. Technol.* , **A4 (3)**, 1035-1038 (1986).

[14]N.J. Dinardo, J.E. Demuth, and T.C. Clarke, "Interaction of Thin Metal Films With the Polyimide Surface: Electron Energy Loss Spectroscopy of Surface Vibrations and UV Photoemission of Electronic States," *Chemical Physics Letters*, **121 (3)**, 239-244, 8 November 1985.

[15] F.S. Ohuchi and S.C. Freilich, "Metal Polyimide Interface: A Titanium Reaction Mechanism," *J. Vac. Sci. Technol.* , **A4 (3)**, 1039-1045 (1986).

CHAPTER 5

EXPERIMENTAL PROCEDURES

INTRODUCTION

A variety of polyimide/metal configurations were considered in order to obtain the best interfacial data. In general, all samples were prepared by spin-coating polyimide solution onto silicon wafers. The desired configuration dictated whether metallization was done before or after polyimide application. Metallizations were done by electron-beam evaporation or dc sputtering. Polyimide curing was done in an N_2-purged environment. The resulting interfaces were studied by infrared and x-ray photoelectron spectroscopy.

TEST STRUCTURE CONFIGURATION

The processing sequence for preparing samples is critical in determining the interfacial characteristics. Due to process limitations samples were exposed to atmospheric conditions between polyimide application and metallization. Thus, careful consideration was given to the effect the process sequence had on the resulting sample geometry and interfacial characteristics. Figure 5-1 shows the two possible geometries from interchanging the spin-coating and metallization steps. Both occur in actual electronic device applications.

As previously suggested, a structure which permitted infrared transmission spectra would be preferred since reference data for bulk polyimide was collected in the transmission mode. However, the high

Figure 5-1. Possible Sample Geometries

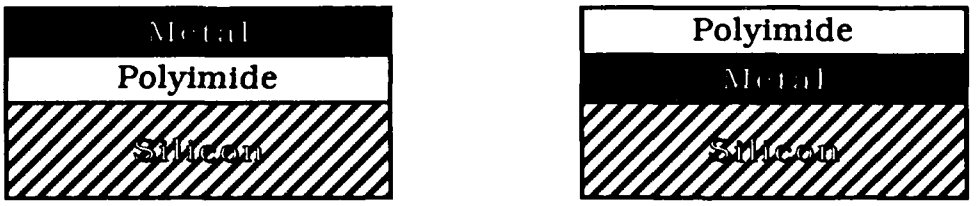

a. Metal on cured PI configuration

b. PI cured on metal configuration

absorbance of metal films prevented the use of transmission techniques in analyzing the polyimide/metal interface. Despite complications from peak shifting due to angular effects, reflection/absorption and attenuated total reflection (ATR) techniques were required.

Reflection/absorption IR requires the material of lower refractive index to be above the one of higher refractive index, as shown in Figure 2-2. ATR techniques require the surface in contact with the internal reflection element (IRE) to have a lower refractive index than that of the IRE, as shown in Figure 2-3. Thus in order to do IR analysis on a structure such as Figure 5-1a, it was necessary to remove the silicon from a structure.

While peeling of 1.1 μm polyimide films from silicon wafers was possible, it was not possible to peel the thinner, metallized films without destroying the structure. Etching holes through the silicon was explored as an alternative approach. Liquid etching with a 23.4 wt% KOH/13.3 wt% isopropyl alcohol/63.3 wt% water provides

orientation-dependent etching of silicon through a patterned silicon dioxide mask. <100>-oriented surfaces are etched with edges at a 54.7° angle from the (100)-surface, while <110>-oriented silicon are etched with straight-walled grooves.[1] The silicon etch rate is relatively high, but once etchant reaches the polyimide it rapidly attacks and penetrates the polymer since polyimides' resistance to alkalis is low.[2]

Plasma etching may also be possible, but in this case the polyimide surfaces show extensive modification of chemical species on the surface.[3,4,5] This could significantly change the IR spectrum for thin films where contributions from the interface, not a modified surface, are of interest.

Since fewer studies have considered the interfacial characteristics which develop during the imidization of polyimide on metals, this work was focused on this industrially important process. While it would have been desirable to obtain IR data on the well-studied metal/polyimide configuration for comparative purposes, the above problems prevented fabrication of a suitable test structure. Thus, the configuration shown in Figure 5-1b was used for both IR and XPS studies of the polyimide/metal interface. Very thin films of polyimide were required for the IR and XPS analyses in order to maximize the signal from the interface and to prevent contributions from bulk materials from masking changes occurring there.

TEST STRUCTURE FABRICATION

Metallization

Metals chosen for the studies were those of interest in the microelectronics industry and covered the range of published polyimide/metal properties. Chromium was chosen as a highly reactive metal which forms strong, sharp, and stable interfaces. Gold forms weak interfaces with polymers, but is relatively stable. While copper also forms weak interfaces, it reacts strongly with polyimide during curing.

The chromium and gold were deposited to a nominal thickness of 1000 Å on silicon wafers using electron-beam evaporation. The films were deposited at 2×10^{-7} torr at a maximum rate of 3 Å/sec. The film thickness during evaporation was monitored and controlled by an Inficon Thin Film Deposition Controller utilizing a quartz crystal thickness sensor. Copper was deposited by dc sputtering at 1×10^{-6} torr to a thickness of 1000 Å. XPS showed the surfaces of the metal films to have significant metal character at the time of polyimide application, although various oxidized states were also present as seen in Figure 5-2. These spectra indicate the type of surface onto which the polyimide films were deposited.

Figure 5-2. XPS Spectra of Metal Surfaces Used in Polyimide/Metal Study

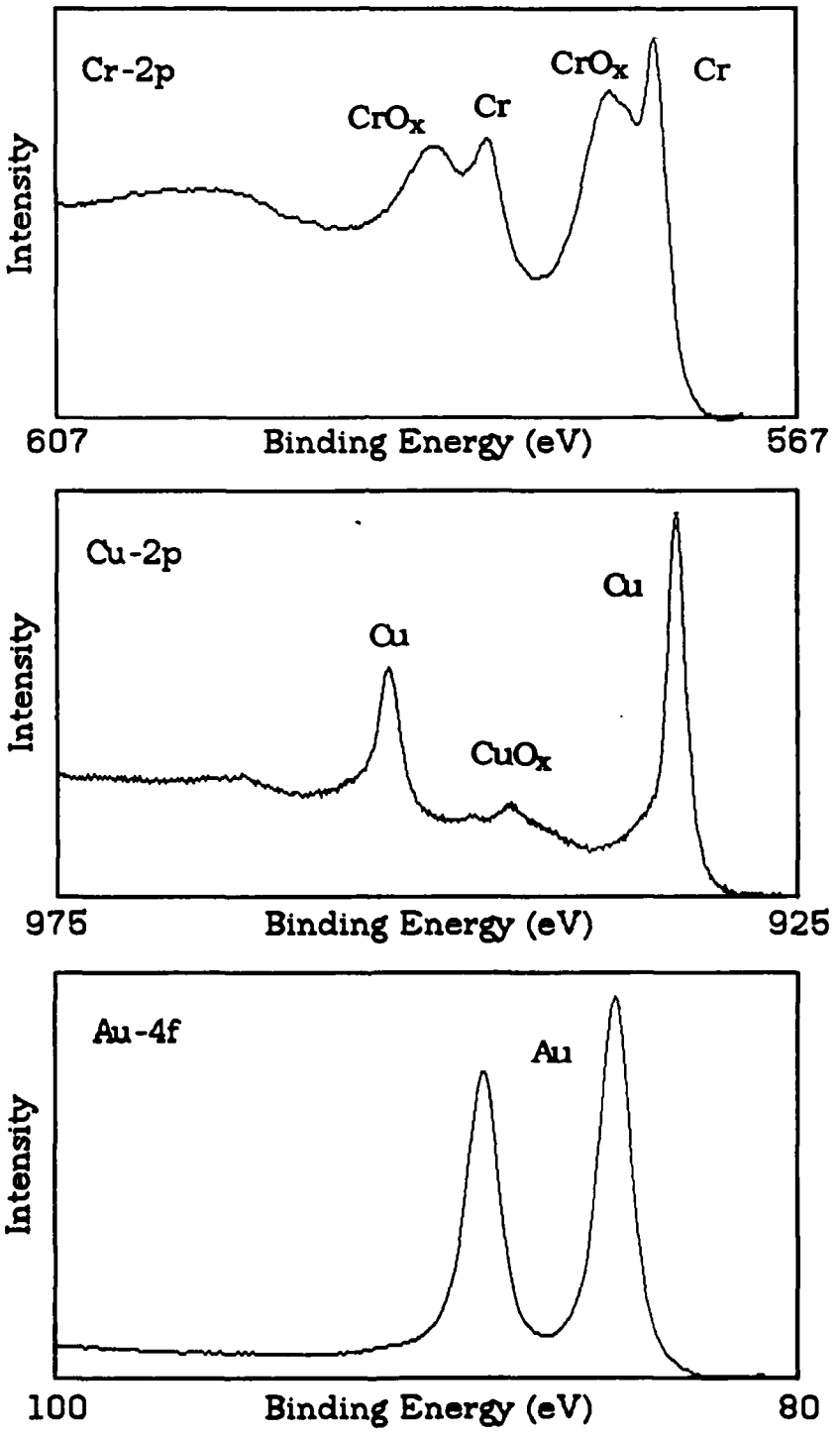

Polyimide Application

Spin Coating

Polyimide was applied using spin-coating of the polyamic acid precursor solution. The final thickness of a spun film is controlled by the solution viscosity and the final spin speed.[6] Spin time is more important to film uniformity across a wafer. Variation in the amount of solution dispensed can cause a variation in average film thickness, but these variations are minimized when high spin speeds are used.[6,7] Static dispensing of the polyimide solution also provides better film uniformity than does dynamic dispensing.[6]

The PI-2545 obtained from the DuPont Company is about 13.5% solids with a viscosity of 9-13 poise.[8] The viscosity can be lowered by diluting the solution with T-9030, a solvent system consisting of N-methyl-2-pyrrolidone and 1-methoxy-2-propanol.[9] Thinned solutions were allowed to stabilize at least 18 hours before processing.

Prior to spin-coating the silicon wafers were baked at 150°C for 30 minutes in a vacuum oven. Wafers were then removed one at a time for spin-coating. A calibrated syringe, to which a 0.2 μm Gelman Sciences Aerodisc CR filter was attached, was used to apply 2 ml of diluted polyamic acid solution to a metallized wafer. This amount of diluted solution flooded a 3-inch wafer. Wafers were then spun at final rates of 2000 to 5000 rpm for 20 to 60 seconds, depending on the desired film thickness. For unthinned solutions approximately 2 ml was poured onto the wafer. The unthinned solutions were too viscous to filter, and pouring them reduced the number of entrapped air bubbles, which if present caused holes in the polyimide films. It was

necessary to distribute the polyamic acid across the wafer at 1500 rpm and rapidly ramp to a final spin speed between 4000 and 5000 rpm.

Polyimide Curing

Immediately after coating, the wafers were placed in a 95°C oven for a 30 minute bake. The polyimide was then cured on an enclosed hot plate which was purged with N_2. The temperature was controlled during the curing to within 2°C of the setpoint.

A variety of cure conditions were used, with final cure temperatures ranging from 250°C up to 400°C. Since higher cure temperatures are known to give better bulk polyimide properties,[2] initially they were used in processing thick films. As thinner films were prepared the polyimide disappeared with 400°C cures, so final cures of 250°C were used for samples in which interface data was obtained. For bulk (thick film) polyimide, no differences were observed in the IR spectra between the 250°C and higher temperature cures, which corresponds with published cure data.[2,10] The temperature ramp rate was 5°C/min.

Film Thickness Measurement

Film thicknesses were measured using a Gaertner Scientific Corp ellipsometer. For thick films the ellipsometer measurements were correlated with α-step profilometer measurements. The ellipsometer was very repeatable for films of μm dimensions; however, day-to- day variations on the same film could be as much as 4% on a 1000 Å film and 14% on a 100 Å film. Once a baseline was established

by measuring samples ranging from 49 Å to 10,100 Å on the same day, calibration samples were then run when determining the thickness of new samples.

Cured PMDA/ODA Film Data

The polyamic acid solutions spin-coated ranged from the supplied 13.5% solids down to a 0.46% solids dilution, which was 1 part PI-2545 : 30 parts T-9039 . Figure 5-3 shows the resulting range of film thicknesses obtained.

Figure 5-3. PI-2545 Thickness vs. % Solids Content

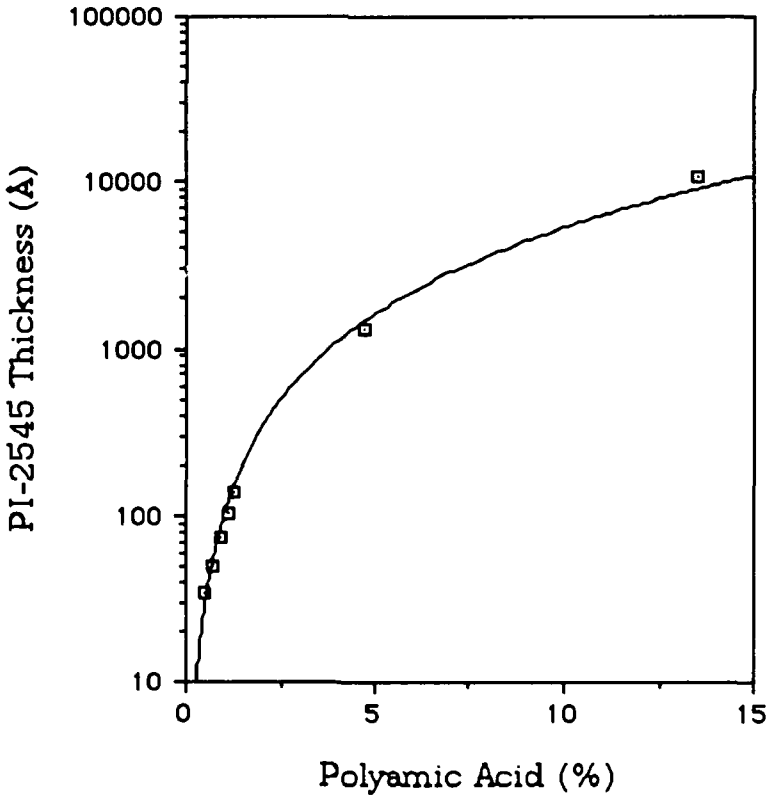

Figure 5-4 shows in greater detail the effect of dilution, spin speed, and spin time on polyimide thickness. It was necessary to develop the thickness curves in the region below 200 Å since the published data[2] has guidelines for obtaining films between 0.5 and 4 μm from dilutions down to only 7.0% solids (1 part PI-2545 : 1 part T-9039). These curves represent solutions having solids contents from 0.46% (1 part PI-2545 : 30 parts T-9039) to 1.1% (1 part PI-2545 : 12 parts T-9039).

Figure 5-4. PI-2545 Thickness vs. Spin Parameters

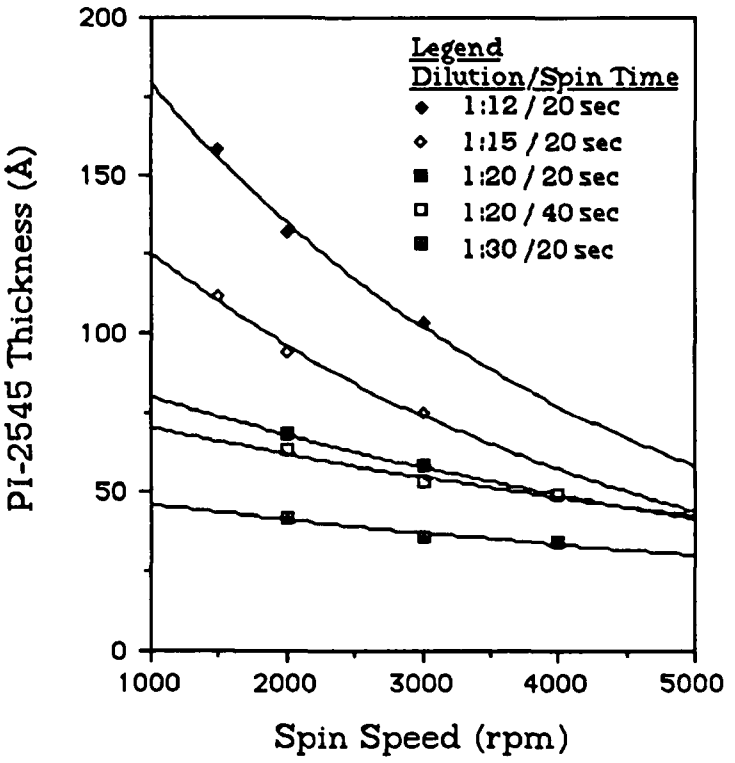

The trends in Figure 5-4 match those seen for higher viscosity solutions giving thicker films: (1) the thickness decreases with increasing spin speed for a given dilution; (2) the thickness decreases with decreasing solids content (lower viscosity) for a given spin speed; and (3) spin time is less important in determining the average film thickness. However, the spin time must be adequate to achieve the desired level of thickness uniformity across a wafer. For example, 20 seconds produced a uniformity of 5.8% thickness variation across a 3-inch wafer for solutions with 0.68% solids, while 40 seconds yielded 3.7% variation. An 8% thickness variation was achieved with a 60 second spin for the 13.5% solids solution.

INFRARED SPECTROSCOPY

The data for this work were collected on an IBM IR/98 FTIR spectrometer, which is a Genzel-type interferometer.[2] The spectra were obtained from 4000-400 cm^{-1} at a resolution of 2 cm^{-1} with a room temperature deuterated triglycine sulfate (DTGS) detector. The mirror velocity was set at 0.166 cm/sec (0.665 cm/sec optical velocity). The optical source was a silicon carbide globar. Computer control established the mirror retardation to attain the desired resolution. Aperture size, which could range from 1.2 mm to 10 mm, and the number of scans collected were a function of the particular sample being analyzed.

The spectra for bulk polyimide films given in Figures 2-4 and 2-6 could be collected with only 500 scans using the 1.2 mm or 2.5 mm aperture. However, the the reflection/absorption and ATR work

on thin films required up to 10,000 scans using the 5mm or 10 mm aperture. In order to obtain spectra with an acceptable signal-to-noise ration, the required scan time was increased with decreasing polyimide thickness. The reflection/absorption spectra were acquired at an incidence angles in the 78-82° range using p-polarized light. For the ATR work the following KRS-5 single pass plates were tried at various times during the research: 45°-50 mm x 10 mm x 3 mm; 60°-50 mm x 10 mm x 3 mm; and 60°-50 mm x 10 mm x 1 mm. The 45° plate provided the most consistent results throughout the mid-IR region .

X-RAY PHOTOELECTRON SPECTROSCOPY

The XPS data for this work were collected on a Perkin Elmer PHI Model 5400 ESCA system. The electron energy analyzer for this system is an hemispherical capacitor analyzer, which can be operated in constant pass energy or constant retarding ratio modes. A constant pass energy of 35.75 eV was used for this work. While a dual anode capability is available, only the magnesium anode was used for this work, operating at 20 mA and 15 kV (300 W). The system pressure during data collection was 5×10^{-10} torr, and an externally adjustable aperture was used top limit the analysis to a 1 mm diameter area.

A few polyimide surfaces were analyzed using the system's angle resolved capability by varying the take-off angle (of electrons relative to the surface) from 10° to 90°. This technique was useful in looking for x-ray damage at the surface during XPS collection and looking for differences in composition as a function of depth. For the

polyimide/metal interface studies, the 90° takeoff angle was used to maximize the penetration depth of the analysis.

For the XPS analysis, 5 mm-square samples were obtained by scribing and breaking the silicon wafer on which the sample had been prepared. An ESCA survey was first collected from 1000-0 eV binding energy to identify the elements present. In a few cases fluorine was detected as a contaminant, the source of which was never found. Following the ESCA survey, detail scans were collected to obtain high resolution bands, which provide the required chemical state identification. The high resolution bands were analyzed for elemental percentage compositions and curve fit to obtain the percentage contributions of various chemical states for each element.

REFERENCES

[1]S.M. Sze, *Semiconductor Devices: Physics and Technology*, John Wiley & Sons (1985).

[2]N.A. Adrova, M.I. Bessonov, L.A. Laius, and A.P. Rudakov, *Polyimides: A New Class of Heat-Resistant Polymers*, Translated from Russian by J. Schmorak, Israel Program for Scientific Translations (1969).

[3] F.D. Egitto, F. Emmi, and R.S. Horwath, " Plasma Etching of Organic Materials. I. Polyimide in O_2-CF_4," *J. Vac. Sci. Technol.* , **B3 (3)**, 893-904 (1985).

[4] M. Kogoma and G. Turban, "Mechanism of Etching and of Surface Modification of Polyimide in RF and LF SF_6-O_2 Discharges," *Plasma Chemistry and Plasma Processing*, **6 (4)**, 349-380 (1986).

[5]N.J. Chou, J. Paraszczak, E. Babich, J. Heidenreich, Y.S. Chaug, and R.D. Goldblatt, "X-ray Photoelectron and Infrared Spectroscopy of Microwave Plasma Etched Polyimide Surfaces, "*J. Vac. Sci. Technol.* , **A5 (4)**, 1321-1326 (1987).

[6]F.L. Givens and W.J. Doughton, "On the Uniformity of Thin Films: A New Technique Applied to Polyimides," *J. Electrochem. Soc.: Solid-State Science and Technology*, **126 (2)**, 269 -272 (1979).

REFERENCES (continued)

[7]DuPont Semiconductor Materials Pyralin Polyimide Coatings, Preliminary Information Bulletin: Spin Coating Techniques, Bulletin #PC-2 (E-69469), Dupont Company, Wilmington, DE (1985).

[8]DuPont Semiconductor Materials Pyralin Polyimide Coatings, PI-2545, Bulletin #PC-9 (E-66037), Dupont Company, Wilmington, DE (1985).

[9]DuPont Semiconductor Materials Pyralin Polyimide Coatings, Product Specification T-9039 Thinner, E-66048, Dupont Company, Wilmington, DE (1986).

[10]Y.K. Lee and J.D. Craig, "Polyimide Coatings for Microelectronic Applications,"*Polymer Materials for Electronic Applications*, edited by E.D. Feit and C.W. Wilkins, Jr., ACS Symposium Series 184, American Chemical Society, 107 -121 (1982).

CHAPTER 6

EXPERIMENTAL RESULTS

INTRODUCTION

The following discussion presents the results of infrared (IR) spectroscopy and x-ray photoelectron spectroscopy (XPS) characterization of PMDA/ODA polyimide and subsequent studies of interfaces it forms with various metals. Data is presented for the polyimide/gold, polyimide/chromium, and polyimide/copper interfaces.

POLYIMIDE CHARACTERIZATION

The PMDA/ODA polyimide used in the polyimide/metal interface studies was characterized by both infrared spectroscopy (IR) and x-ray photoelectron spectroscopy (XPS). For clarity in discussing the experimental results, the PMDA/ODA chemical structure is given in Figure 6-1.

Figure 6-1. PMDA/ODA Polyimide Structure

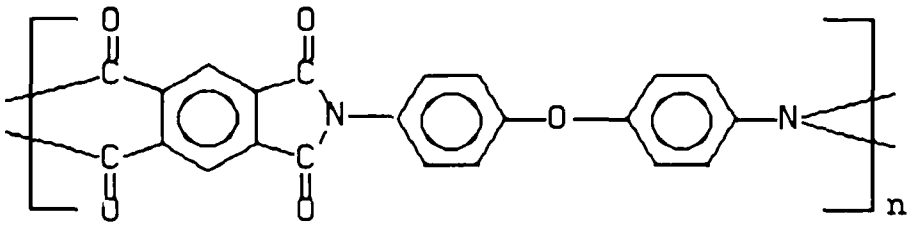

PMDA / ODA Polyimide
Poly[N,N'-bis(phenoxyphenyl)pyromellitimide]

Figure 6-2 shows the IR spectrum of 1.1 μm PMDA/ODA films at various stages of imidization. The strongest absorption peaks are identified by the responsible chemical structures. Curve (a) is the spectrum of polyamic acid, while curve (c) is typical of the PMDA/ODA polyimide. Curve (b) shows a partially cured sample, which has characteristics of both the polyamic acid and the polyimide. These samples were prepared by spin-coating the PI-2545 onto a silicon wafer and cured as shown. The resulting 1.1 μm film was removed from the wafer after soaking the film in deionized water. As was discussed in Chapter 3, the polyamic acid characteristics at 1659 cm^{-1} and 1535 cm^{-1} decrease during curing, while polyimide peaks emerge at 1776 cm^{-1}, 1377 cm^{-1}, and 725 cm^{-1}. These IR spectra will be useful in discussing the changes which are observed with the polyimide/metal interactions.

Cure studies with IR showed one hour at 250°C fully imidized the PMDA/ODA precursor. IR could not detect any difference in bulk material spectra with higher temperature cure schedules. Intermediate curing steps at lower temperatures did not have a significant impact on the final cure state.

Figure 6-2. IR Spectra of PMDA/ODA During Imidization

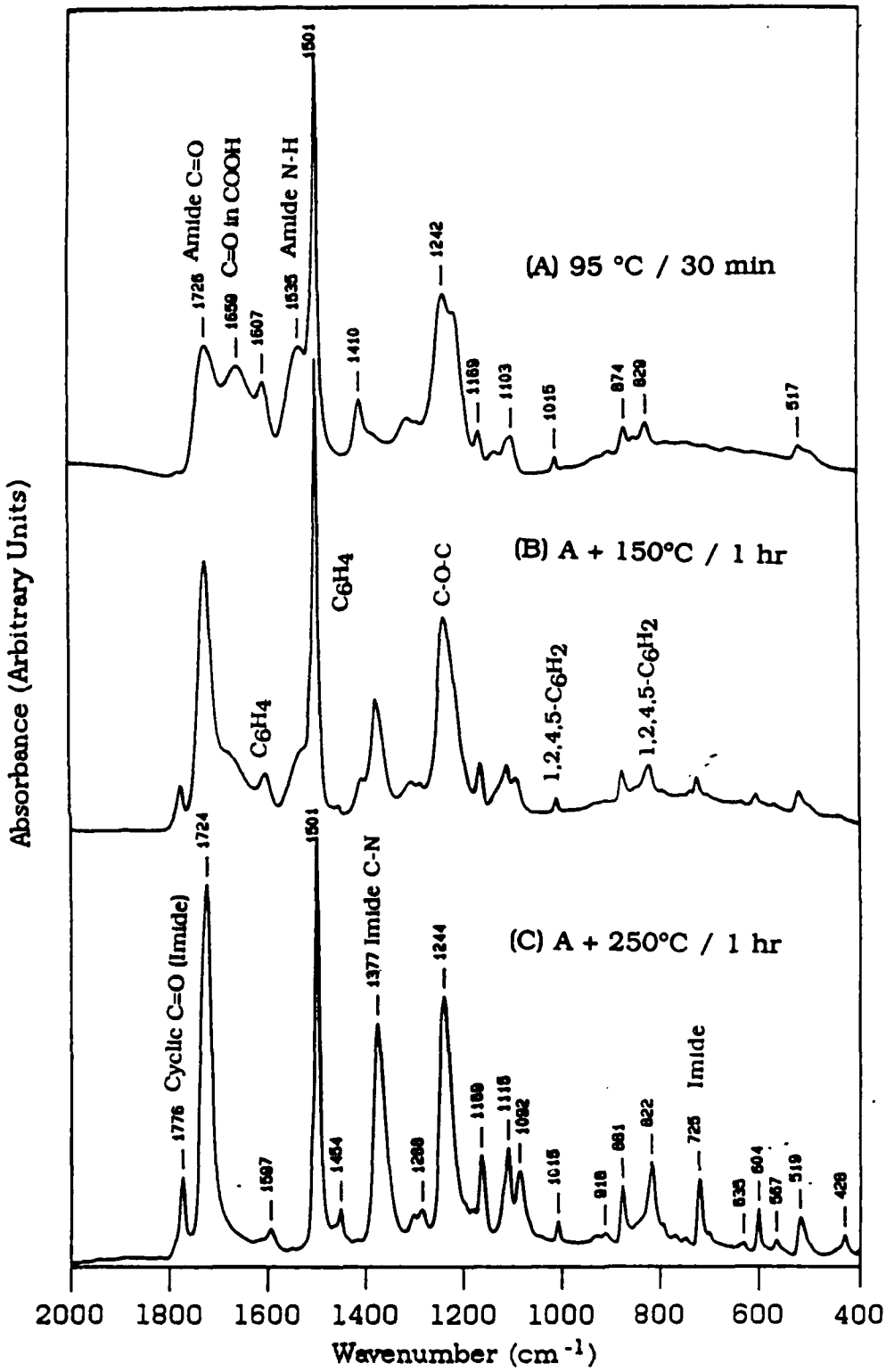

Figure 6-3 shows the effect the reflection/absorption (RA) technique has on the polyimide IR spectrum. This IR spectrum was collected in the RA mode from a 1.1 μm polyimide film cured on gold metallization. By comparing Figures 6-2 and 6-3, one sees the C=O region for the RA spectrum has an additional peak at 1744 cm^{-1}. As was discussed in Chapter 2, the RA technique can shift bands to higher wavenumbers for thin films. In the polyimide/metal data which is presented later for 34 Å to 1328 Å polyimide films, the C=O band at 1724 cm^{-1} in transmission is completely shifted to the 1740 cm^{-1} region by the RA technique.

Figure 6-3. RA Spectrum of 1.1 μm Polyimide on Gold

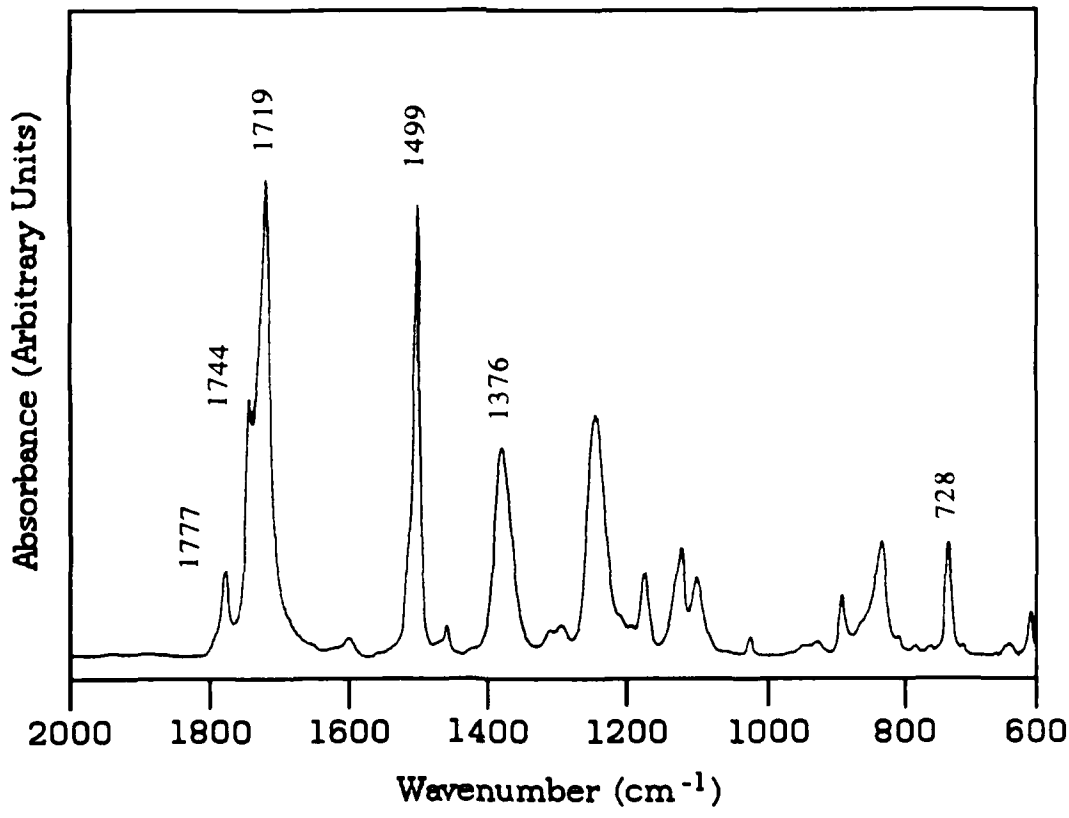

Figure 6-4 shows the C-1s, N-1s, and O-1s XPS spectra for the surface of a 140 Å PMDA/ODA film on gold. Anderson *et al* [1] showed polyimide films of this thickness exhibit negligible charging effects. The spectra have been fitted with Gaussian-Lorenzian peaks to show contribution from the various electronic states. One should note that these fitted bands are not unique, but were selected using published data as guidance. By comparing the data in Table 6-1 with the published results summarized in Table 3-2, one observes that the absolute location of the C-1s band is slightly downshifted from the published data. However, the relative location (ΔBE) of the synthesized components are within the range of previously reported data. Anderson *et al* [1] noted that the slight discrepancies in reported

Table 6-1. Summary of PMDA/ODA XPS Results

Band & Components	Binding Energy (eV)	ΔBE (eV)	Relative Percent Experiment	Predicted
C-1s				
C-C	284.4	0	36.8	36
C-O,C-N, & PMDA C-C	285.5	1.1	49.0	46
C=O	288.4	4.0	14.2	18
N-1s				
	399.0	(1.5)	2.8	
Imide	400.5	0	97.2	100
O-1s				
C=O	532.1	0	69.0	80
C-O	533.4	1.3	31.0	20

Figure 6-4. XPS Bands of PMDA/ODA Polyimide

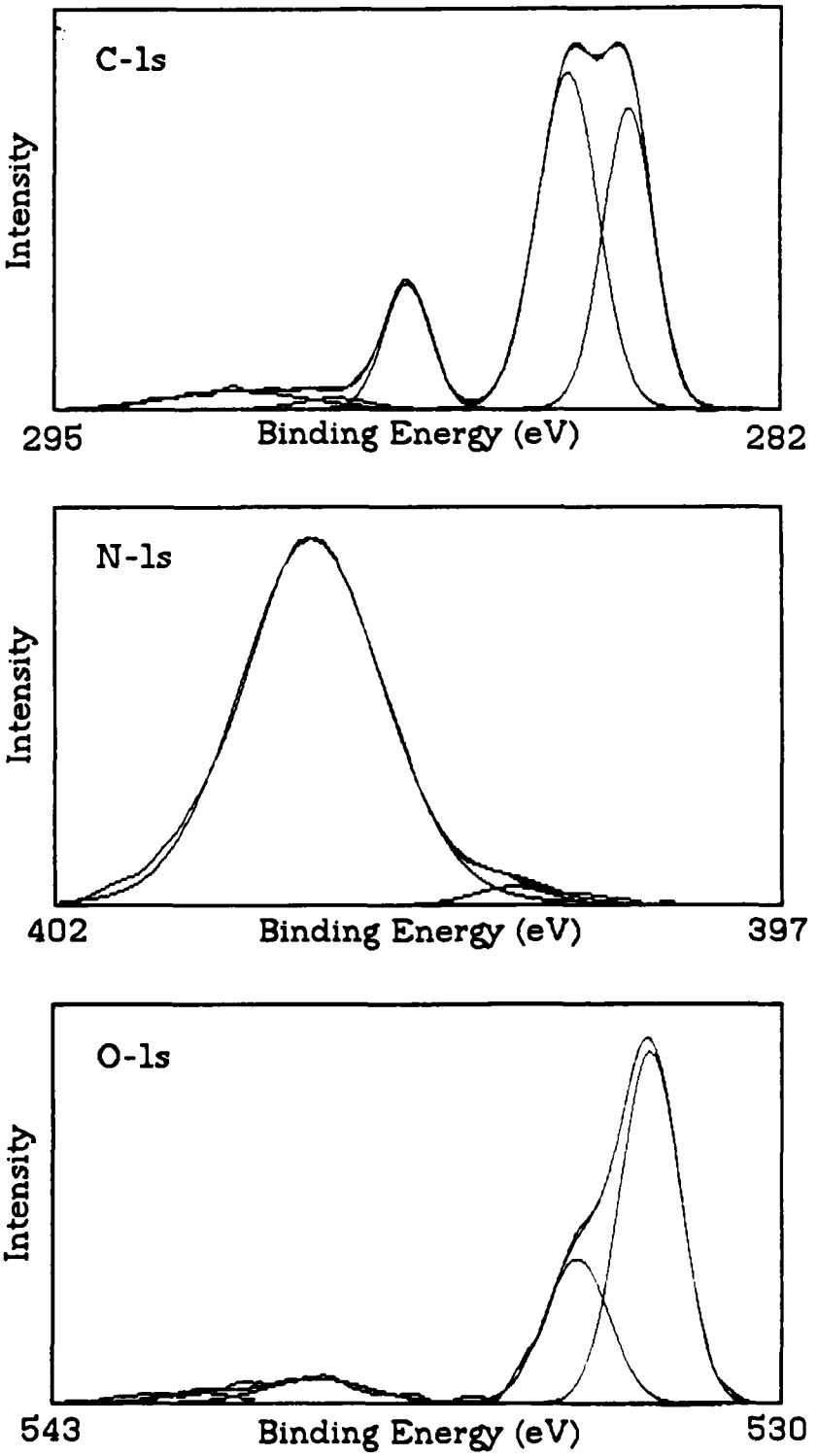

core level positions for thin films may be attributed to differences in heat treatment, since different heat treatments would modify the number and density of defect states in the polyimide. Since the Fermi level of the polyimide is pinned by defect states, shifts would occur in the core level binding energies.

The C-1s and O-1s regions indicate carbonyl deficiencies exist at the surface of the polyimide, when compared to the ratios expected for the PMDA/ODA polyimide shown in Figure 6-1. Previous experimental work found 13.2-15.0% of the C-1s band and 69.7-73.0% of the O-1s band were attributable to carbonyl. Thus, the carbonyl deficiency is in agreement with published results.

Two N-1s binding states were observed, and angular resolved XPS at 15°, 45°, and 90° take-off angles did not show significant differences in relative contributions of the components. Components in the 399.0 eV region have been assigned to nitrogen double-bonded to carbon or to hydrogenated nitrogen.[1] If isoimide, which has a C=N structure, is the source of the second N-1s peak, it is present at the surface of the polyimide with the amount remaining constant throughout the depth probed by XPS.

Tests were also run to ensure polyimide modification during exposure to x-rays was negligible during the time required to collect a spectrum. After eight hours of exposure, less than five percent change was observed in the characteristic PMDA/ODA C-1s, N-1s, and O-1s spectra.

POLYIMIDE-GOLD INTERFACE

The polyimide/gold system was chosen for this work as the system which was expected to be inert. Meyer *et al* [2] found no evidence of chemical interactions between gold and polyimide when conducting *in situ* XPS studies on the evolution of the gold/polyimide interface. Both IR and XPS studies were conducted for polyamic acid films imidized on gold-metallized wafers.

Figure 6-5 presents the IR-RA results for 1328 Å, 140 Å, and 34 Å PMDA/ODA films with a final cure at 250°C for one hour. The structures were studied with both RA and attenuated total reflection (ATR) techniques, with RA yielding results with the best signal-to-noise ratio (SNR).

The three spectra in Figure 6-5 have the characteristics of bulk polyimide when compared to curve (c) in Figure 6-2 and show no significant changes as successively thinner polyimide films are sampled. As previously stated, the C=O band at 1724 cm^{-1} in the transmission spectrum is shifted to 1741 cm^{-1} by the RA technique.

The XPS C-1s, N-1s, and O-1s bands for 140 Å and 34 Å polyimide films on gold are shown in Figure 6-6. Gold was not detected for the 140 Å structure, but a strong Au-4f band typical of pure gold was observed for the 34 Å film.

The differences between the bands for the two film thickness are very small. Figure 6-7 shows the changes which occurred in the C-1s band as a function of polyimide thickness. As films became thinner the aromatic carbon component at 284.4 eV increased, while the component at 285.5 eV for C-O, C-N, and imide ring carbons

Figure 6-5. IR Spectra of PMDA/ODA-Gold

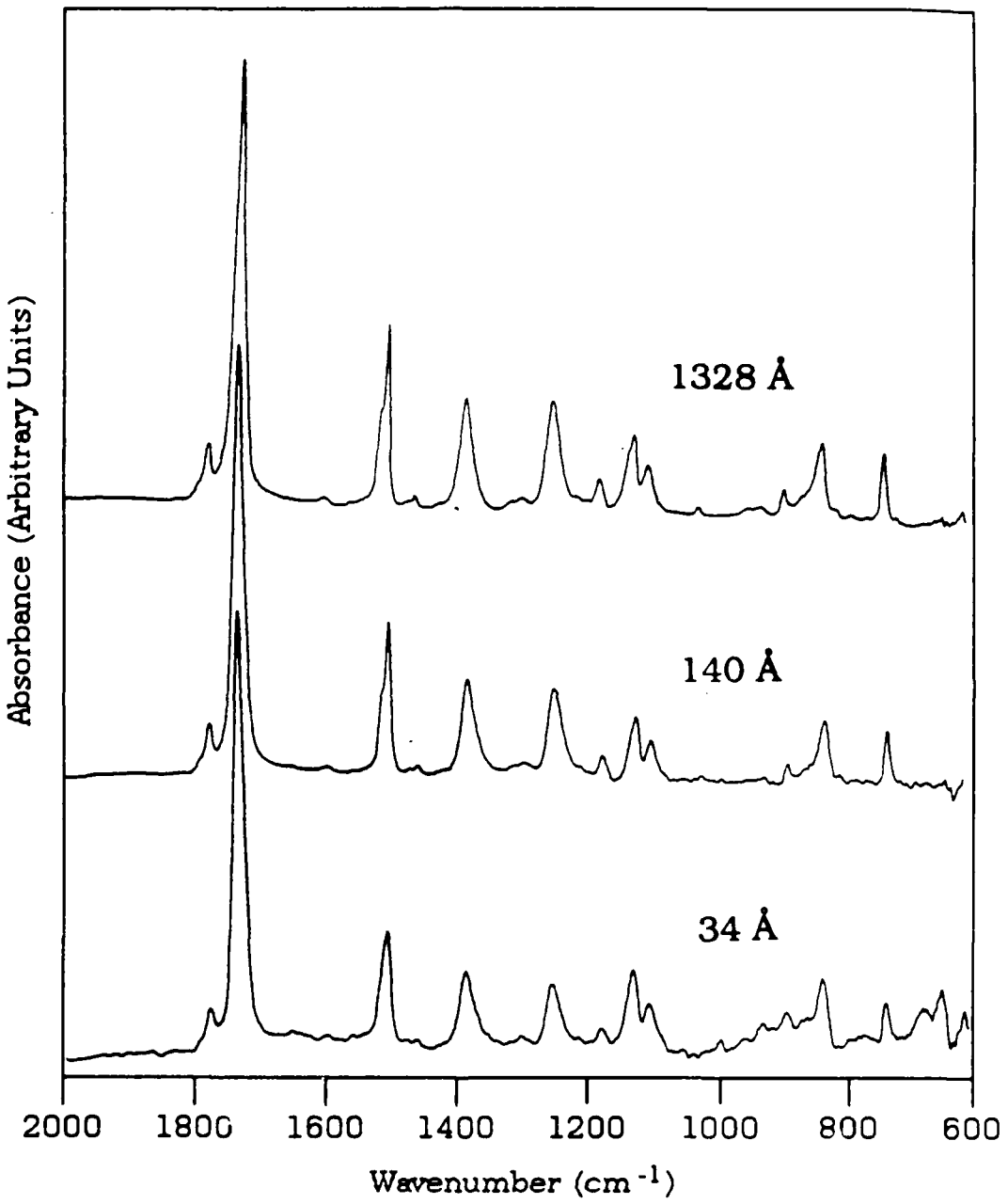

Figure 6-6. XPS Bands of PMDA/ODA on Gold

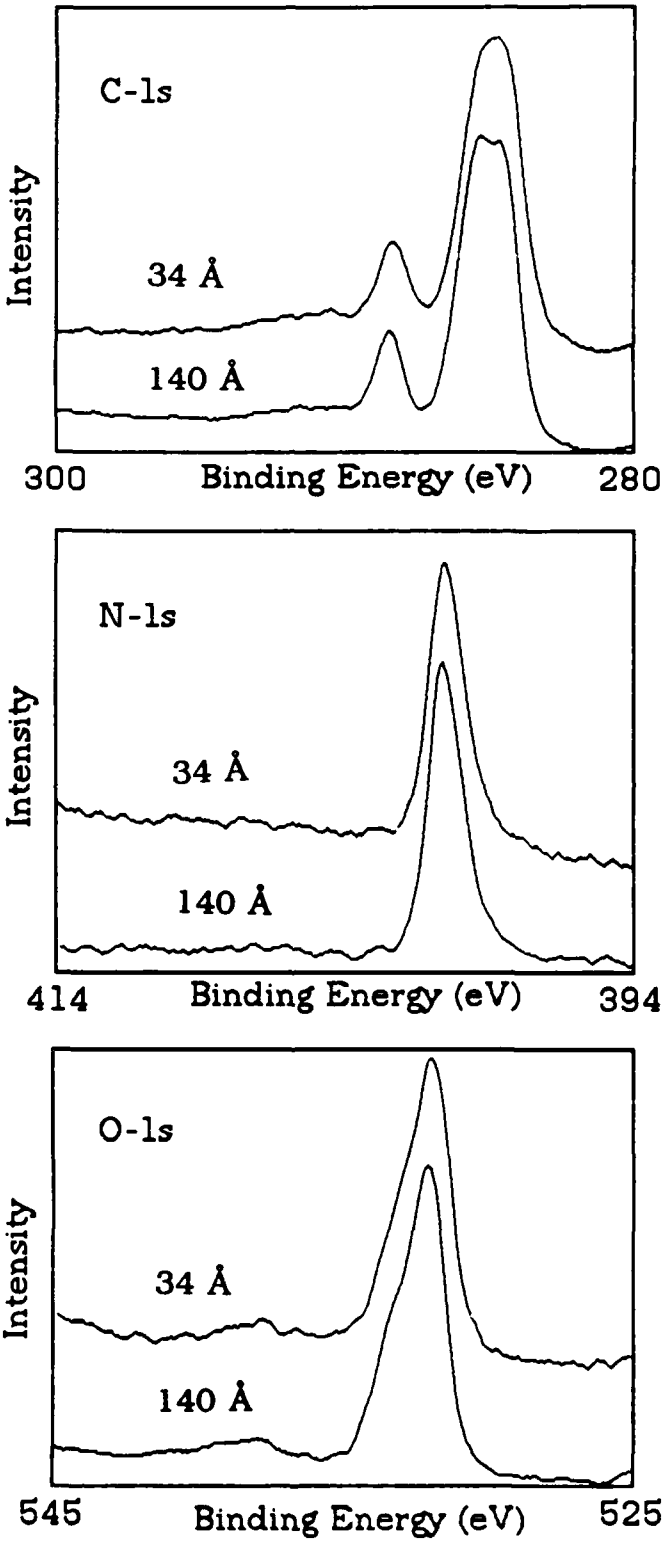

Figure 6-7. Changes in C-1s Band for Polyimide/Gold

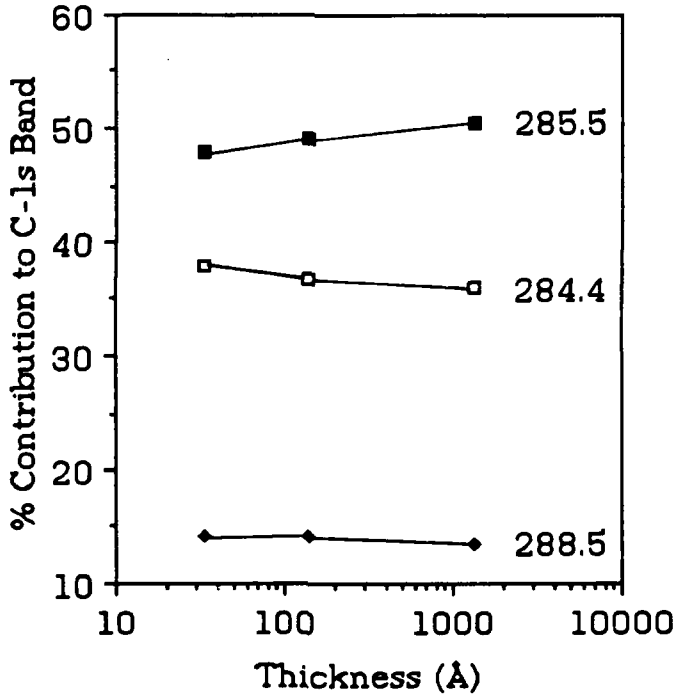

decreased. The carbonyl contribution remained constant. This change in component band contributions could be explained by gold interacting with the PMDA/ODA chain at the imide linkage, reducing the electron withdrawing character of the C=O groups. As a result, the PMDA carbons' contribution to the C-1s band is shifted down to the aromatic region of the band. This mechanism was proposed by Jordan *et al* [3] to explain similar trends for chromium deposited on polyimide.

POLYIMIDE- CHROMIUM INTERFACE

The PMDA/ODA-chromium system was chosen because of chromium's usage as an adhesion layer with polyimide and because of the extensive *in situ* XPS studies depositing chromium onto cured polyimide.

Both the IR and the XPS results for polyamic acid films imidized on chromium-metallized wafers were very similar to the polyimide on gold results. Figure 6-8 contains the IR-RA results for 1328 Å, 140 Å, and 34 Å PMDA/ODA films on chromium. As with the gold films, the structures were studied using both RA and ATR techniques, with the RA spectra having the better SNR. Again, no significant changes were observed as thinner polyimide films were analyzed.

It should be noted that the noise which was evident below 1000 cm^{-1} in the 34 Å film on gold, is more of a problem with the 34 Å film on chromium. Although the 725 cm^{-1} imide peak can be seen in this low wavenumber region, the noise limits the useable spectrum region for thin films to wavenumbers above 1000 cm^{-1}.

Figure 6-9 shows the XPS bands for 140 Å and 34 Å polyimide films on chromium. No chromium was detected when the 140 Å film was analyzed, but a strong Cr-2p band with mostly oxide character was found with the 34 Å film. Chromium was first observed with a 75 Å polyimide/chromium structure. Metallic chromium was evident in each of the spectra for which the metal was detected.

Figure 6-8. IR Spectra of PMDA/ODA-Chromium

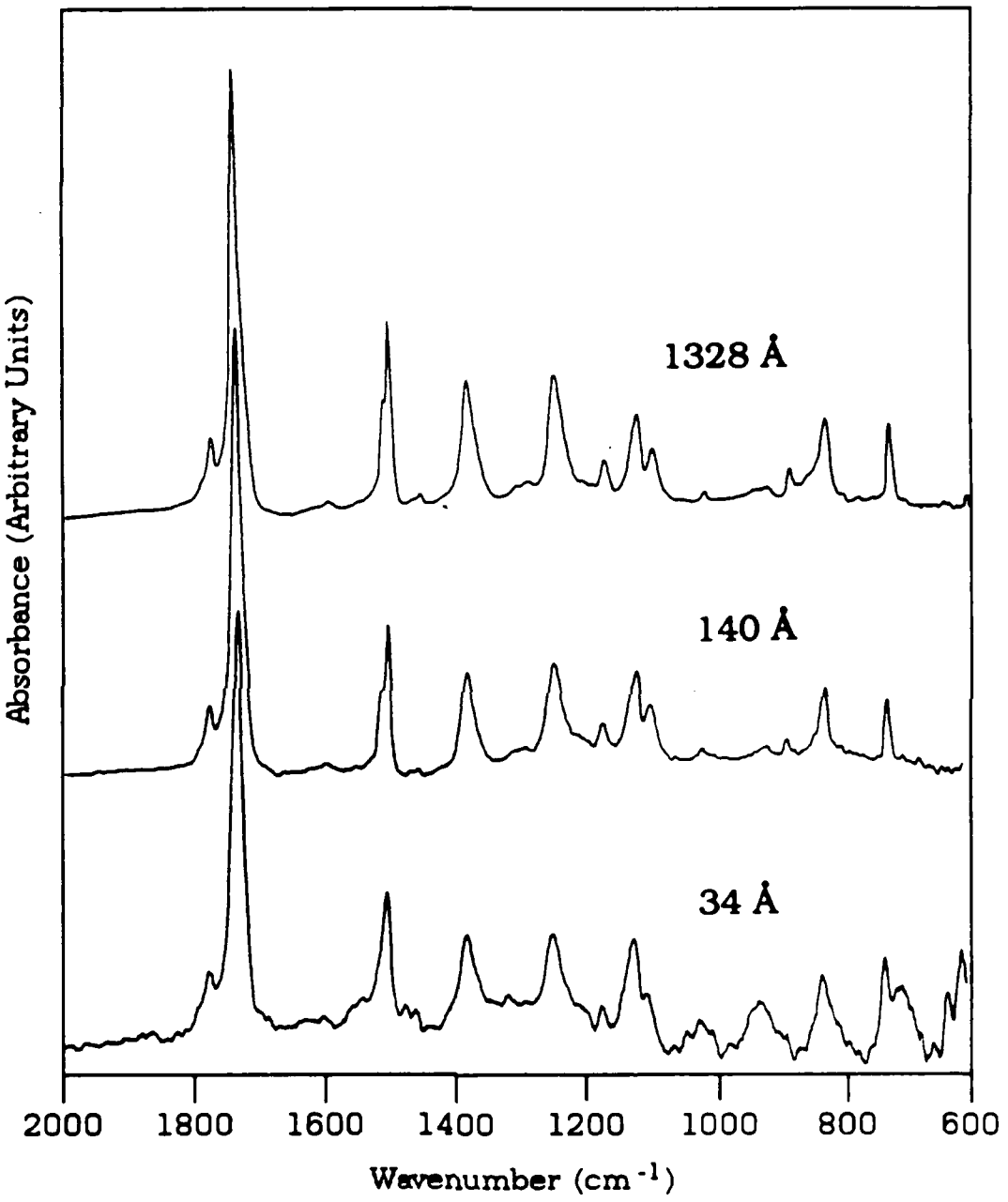

Figure 6-9. XPS Bands of PMDA/ODA on Chromium

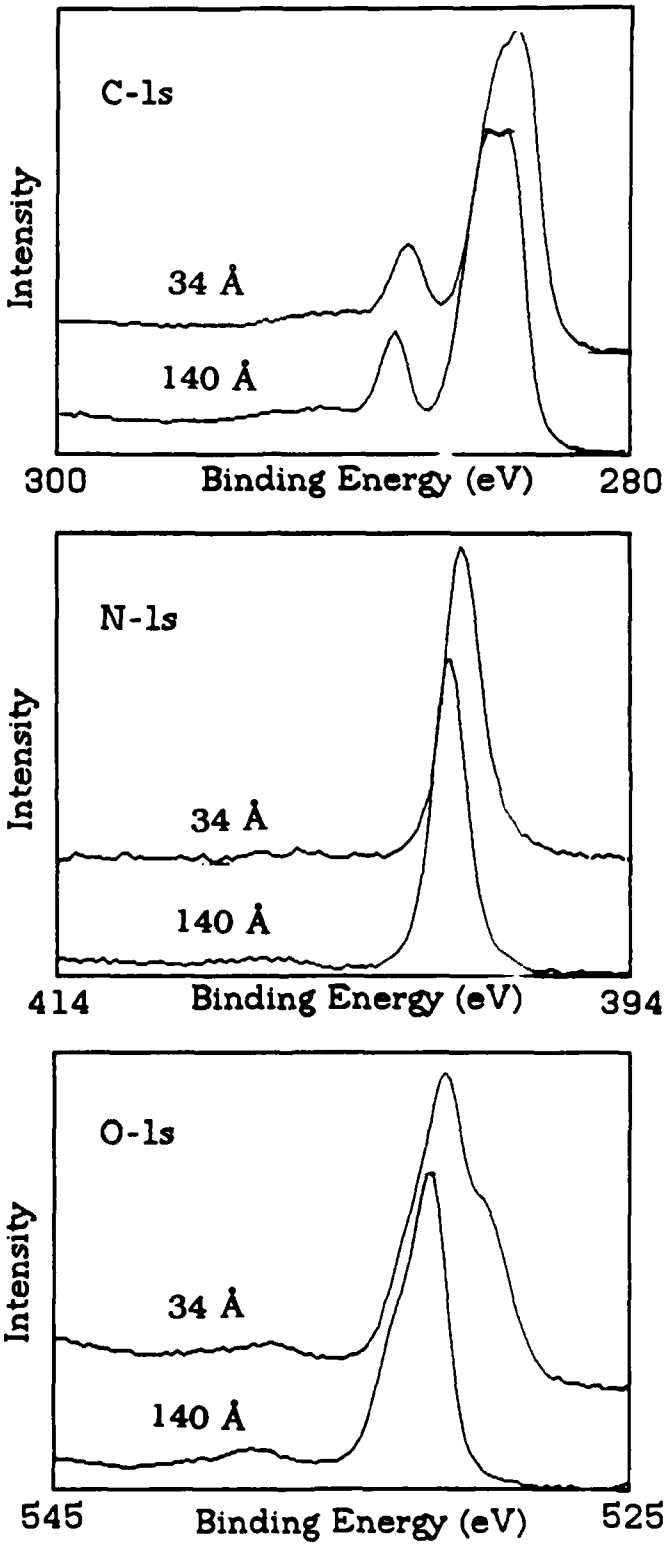

Only small changes were observed in the C-1s band, as shown in Figure 6-10. The trends are almost identical to those found for the the polyimide/gold system suggesting the chromium may be interacting with the carbonyl groups and influencing the electronic structure of the PMDA aromatic ring. The O-1s band for the 140 Å film is typical of polyimide, .while the O-1s band for the 34 Å film has a significant lower binding energy component attributable to chromium oxide species. The complexity of the chromium oxide region makes component analysis of the O-1s band difficult with the results dependent on the initial estimates of the type and quantity of contributing oxide species.

Figure 6-10. Changes in C-1s Band for Polyimide/Chromium

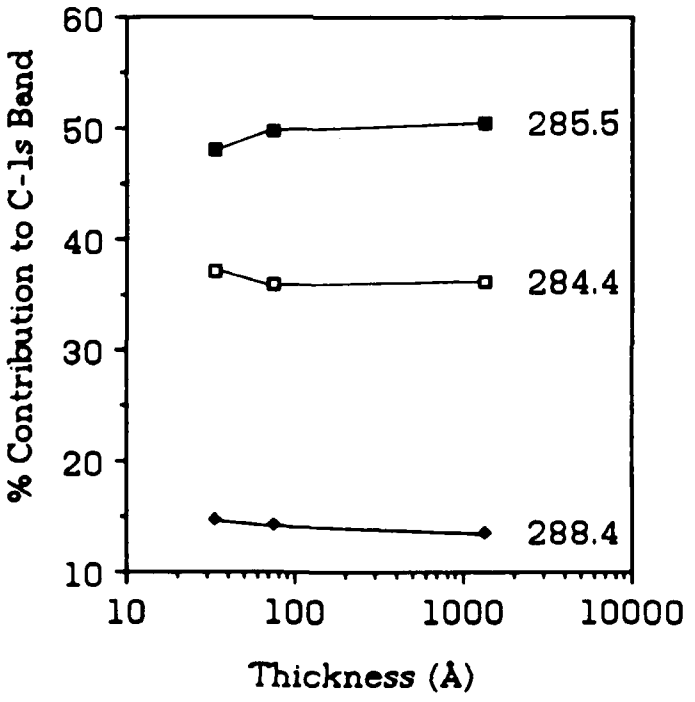

In Figure 6-9 a downshift is observed in the XPS bands for the 34 Å film. Anderson *et al* [1] observed similar downshifts when studying the curing and degradation of polyimide on aluminum. The downshift was observed during curing, and further downshifts occurred during the degradation process. Anderson *et al* attributed this to the modification of polyimide defect states which, as previously discussed, pin the polyimide Fermi level.

POLYIMIDE-COPPER INTERFACE

The RA spectra for successively thinner PMDA/ODA films on copper are given in Figure 6-11. The spectra given are for films thicknesses of 1328 Å, 140 Å, and 34 Å. Contrary to the results obtained with gold and chromium, significant changes are observed in the IR spectra. The changes are apparent on the 1328 Å film and become stronger with thinner films.

Figure 6-12 is useful in considering the changes which occur with the polyimide/copper system. This figure presents the 140 Å film spectra from 1900 to 1300 cm^{-1} for gold, chromium, and copper. Compared to the polyimide/gold and polyimide/chromium spectra, four features develop in the polyimide copper spectrum:

1. In the carbonyl region a peak emerged at 1674 cm^{-1}, just below the standard polyimide C=O doublet.
2. The peak at 1603 cm^{-1} became stronger.
3. A shoulder emerged on the high wavenumber side of the 1501 cm^{-1} peak.
4. The 1377 cm^{-1} imide peak developed into a doublet for the polyimide/copper structure.

Figure 6-11. IR Spectra of PMDA/ODA-Copper

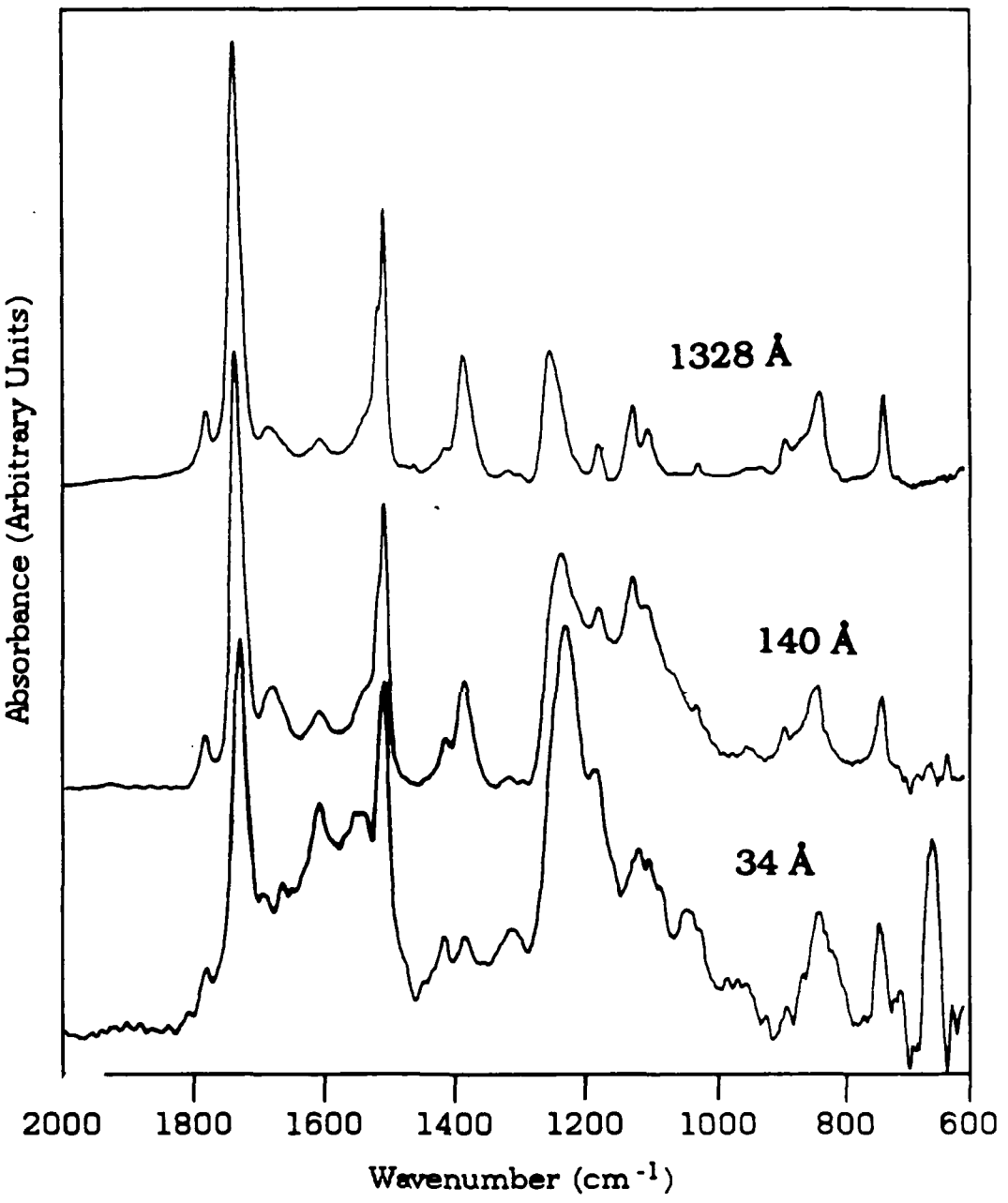

Figure 6-12. IR Spectra Changes for 140 Å PMDA/ODA on Au, Cr, and Cu

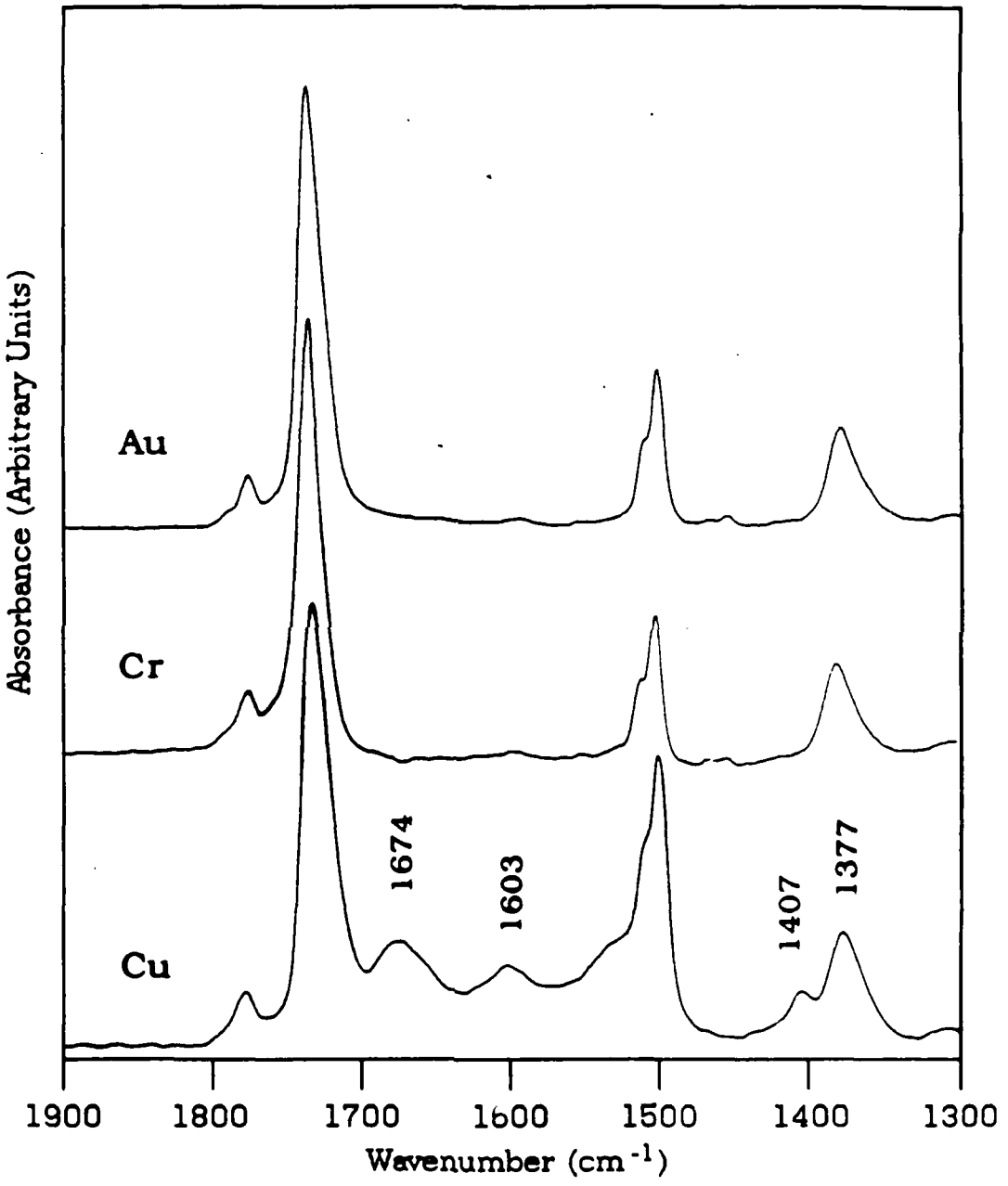

By comparing these peaks with those of polyamic acid in Figure 6-2, it is apparent that polyamic acid type chemical structures are contributing to the polyimide/copper IR spectra. The 1674 cm^{-1} peak is typical of the carbonyl group found in the carboxylic acid functionality in the polyamic acid precursor. The peak at 1603 cm^{-1} is for the aromatic rings in the ODA segment of the polymer. While this structure is present in both polyimide and polyamic acid, the absorption is relatively stronger in the polyamic acid as seen in Figure 6-2, and can be detected above the background only for thicker polyimide films. The shoulder on the 1501 cm^{-1} peak is in the region of the amide N-H vibration, while the peak at 1407 cm^{-1} is also a polyamic acid peak.

These findings compare favorably with those of Kelley *et al* [4] who studied the effects of on much thicker polyimide films than used in this work. They used 1000 Å polyimide films cured on copper in air and nitrogen. In the air-cured films, they observed both curing and degradation occurring simultaneously, with nitrile and oxide products beginning to emerge after one hour at 250°C. The reported spectrum for the one hour cure in air is very similar to the 34 Å spectrum shown in Figure 6-11 which was obtained with a one hour, 250°C cure in nitrogen. The broad absorption band in the 1800-1500 cm-1 region of Figure 6-11 developed into a single broad band upon further curing in the work of Kelley *et al.* [4] Other changes in the IR spectra, including developing nitrile and copper oxide peaks, with further 250°C temperature exposures were attributed to ring cleavage. No

nitrile was detected in the spectra shown in in Figure 6-11, but copper oxide was detected at 650 cm^{-1}.

Kelley *et al* [4] did not observe degradation products for films cured on copper in nitrogen or for films cured on chromium in air. For nitrogen-cured polyimide/copper structures, the IR spectrum was typical of partially-cured, undegraded polyimide. Their spectrum obtained by the metal overlayer technique for a 400 Å film appears identical to the 1328 Å spectrum in Figure 6-11. The metal overlayer technique increased the sample absorptivity by an order of magnitude over ordinary RA. Their published RA spectrum for a two hour, 250°C cure of a 1000 Å film shows much more polyamic acid character than does the corresponding 1328 Å curve in Figure 6-11. This may indicate further incorporation of the copper into the polyimide matrix with increased time at elevated temperature. Tromp *et el* [5] and Kowalczyk *et al* [6] have published results discussing the diffusion of copper in polyimide.

Both studies showed that copper has significant mobility in polyimide, both during and after curing. Tromp *et al* [5] showed that for deposition of copper at successively higher temperatures onto cured polyimide films, the copper diffused deeper into the polyimide. More directly related to this study, Kowalczyk *et al* [6] showed solvent played a significant role during the curing of polyamic acid. When solvent-free films were prepared by molecular beam deposition and cured in nitrogen, a sharp polyimide/copper interface was formed. However, with solvent present, copper precipitates formed and diffused to a region about 500 Å from the interface.

The XPS data for the PMDA/ODA-copper system is shown in Figure 6-13. Copper was detected in the 140 Å film. By comparing this figure with the polyimide/gold bands in Figure 6-6, one sees significant changes have occurred in the polyimide/copper system. These changes are seen better when Figures 6-14 and 6-15 are considered.

Figure 6-14 contains information from the curve fitting of the C-1s bands. Even with the 1328 Å film, increased 284.4 eV contribution and decreased 285.5 eV contribution are observed. The trends are the same as for the gold and chromium systems, but occur at a faster rate.

Figure 6-15 contains curve-fitted XPS bands for the 34 Å film. By comparing these bands with the polyimide reference bands in Figure 6-4, one sees rather drastic changes have occurred, even with the 140 Å film. Similar changes were observed by Anderson *et al* [1] their curing and degradation study.

As previously discussed, the band downshifting is likely caused by a change in the defect states of the polyimide. With changes in the shape of the core level bands indicating a change in the chemistry of the polyimide, one would expect the defect states to change also.

Anderson *et al* [1] found a decrease in the carbonyl functionality in the C-1s band, which reduces the electron withdrawal from the PMDA ring carbons. As a result, the aromatic carbon feature is enhanced. These trends can be seen for the polyimide/copper interface by comparing Figures 6-4 and 6-15

Figure 6-13. XPS Bands of PMDA/ODA on Copper

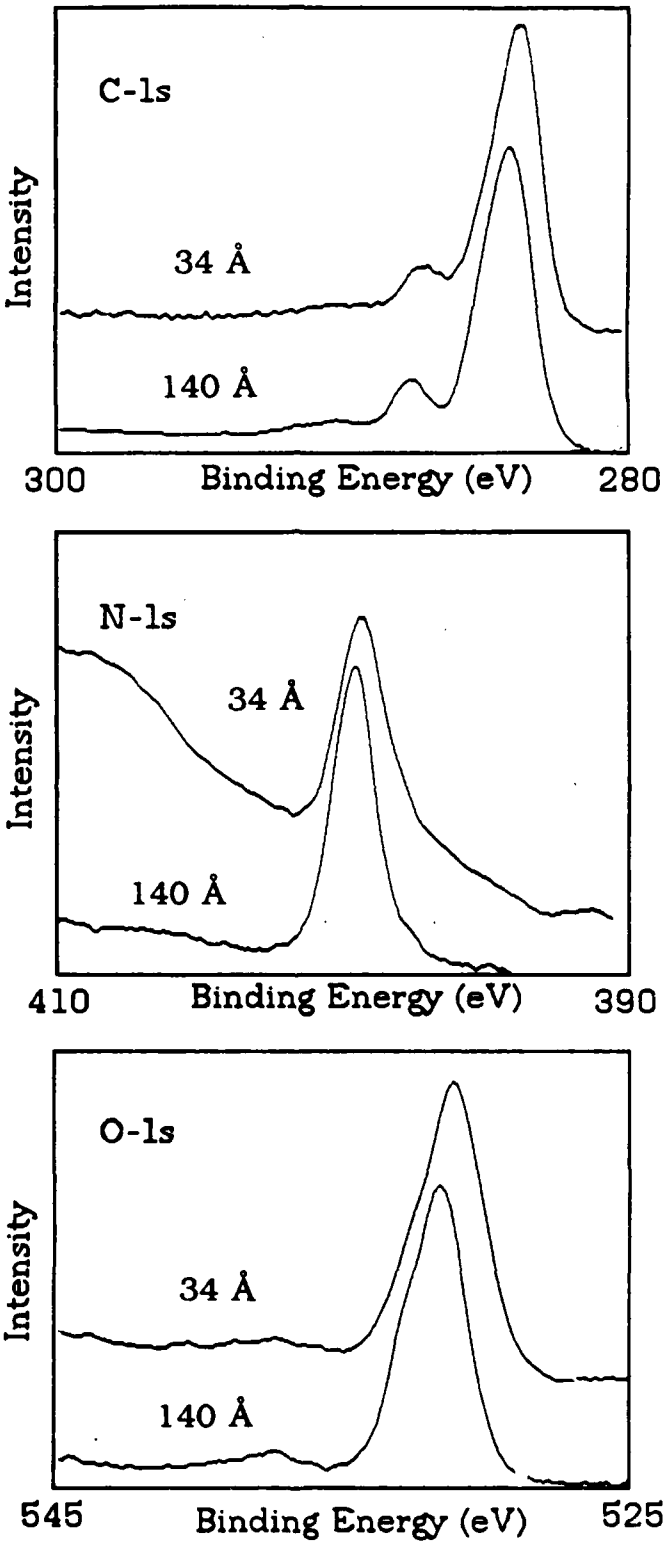

Figure 6-14. Changes in C-1s Band for Polyimide/Copper

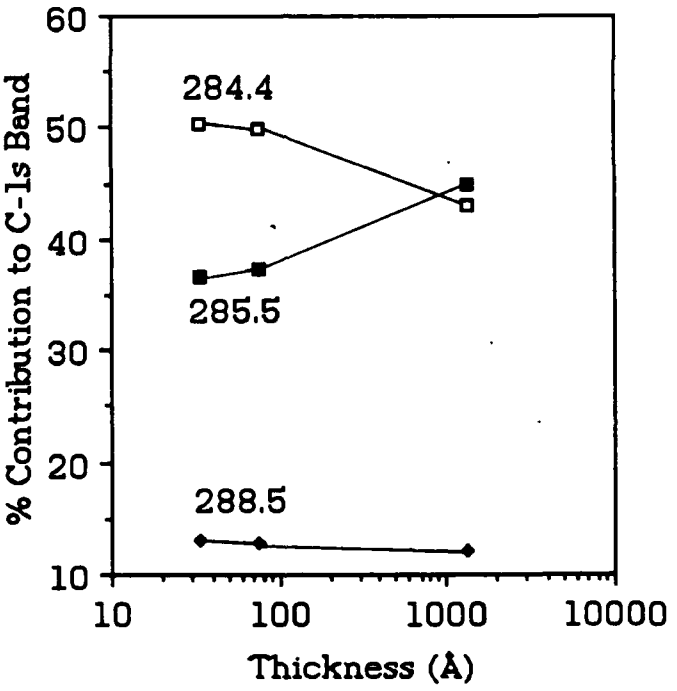

Figure 6-15 Fitted XPS Bands for 34 Å PI on Cu

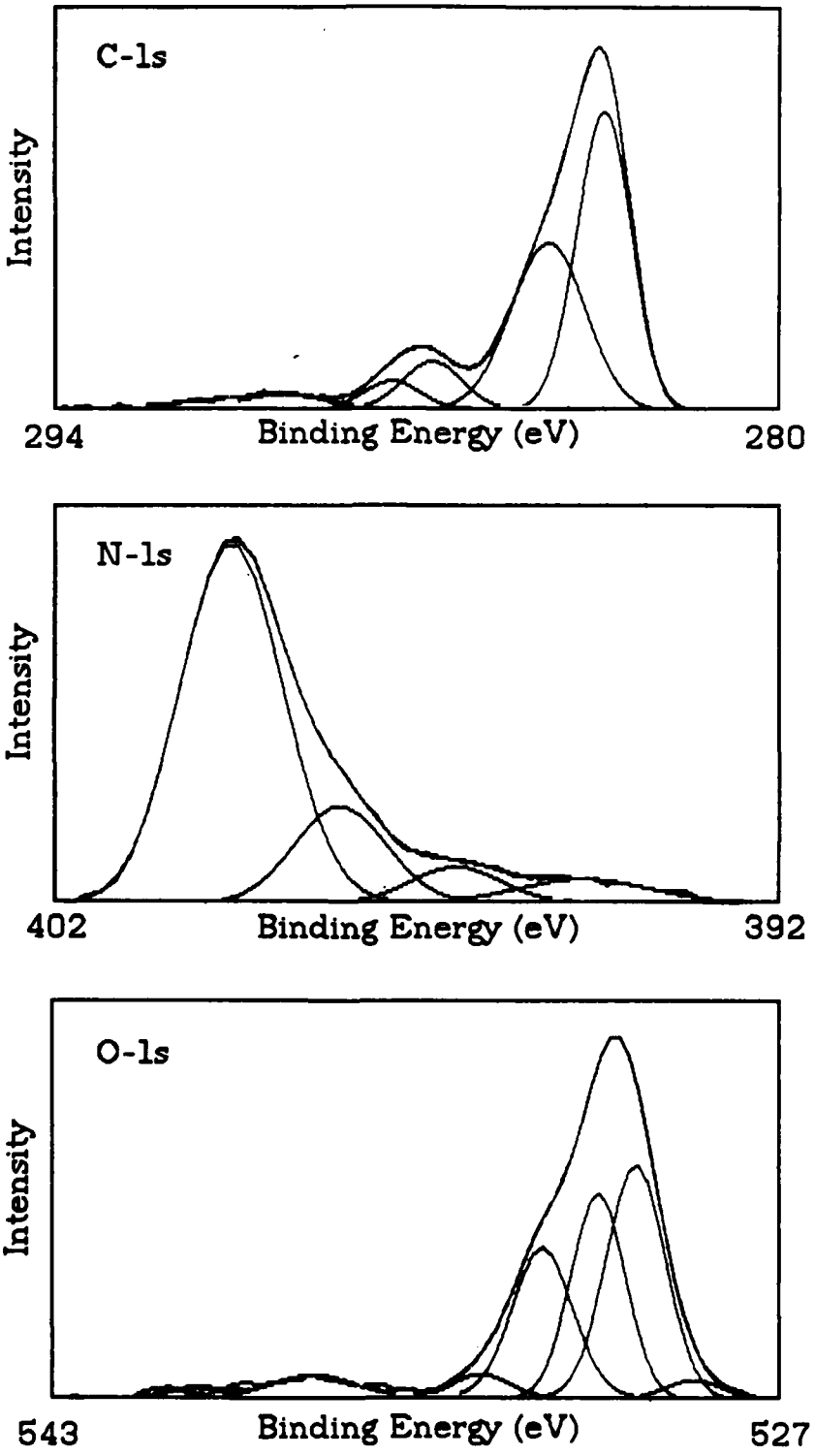

Possibly the most significant XPS result is the emergence of lower binding energy components in the N-1s band. Anderson *et al* [1] reported two lower binding energy N-1s components for polyimide films exposed to high temperatures. The first component was assigned to double-bonded nitrogen or hydrogenated nitrogen, while the second to triple-bonded nitrogen. The presence of low binding energy components is not typical of the amide functionality, which contradicts the proposal by Kelley *et al* [4] that nitrogen-cured films on copper do not degrade. The changes in the N-1s band indicate the imide ring is being cleaved.

As with chromium, a metallic copper component could be seen in each case where copper was detected. This corresponds well with the research by Kowalczyk *et al* [6] since the formation of copper precipitates which diffuse into the polyimide would process would continue to expose metallic copper.

CURE TEMPERATURE EFFECT

Cure temperatures as high as 400°C in nitrogen were studied with polyimide/chromium structures. These cure schedules were initially explored because, as discussed in Chapter 3, some properties are optimized with higher final cure temperatures for the polyimide. For films down to 1000 Å films the IR and XPS data showed typical polyimidc character. As thinner films were deposited, however, it became evident that the polyimide was not withstanding the higher temperature excursions. Initially these films cured at 250°C exhibited IR and XPS survey spectra indicative of polyimide. However, with the

additional 400°C cure, the polyimide character disappeared and strong chromium and oxygen peaks emerged.

Figure 6-16 shows the IR spectra of: (a) a 100 Å PMDA/ODA film on chromium cured in nitrogen at 250°C for 1 hour and at 400°C cure for 30 minutes; and (b) a chromium surface oxidized in air at 400°C for 1 hour. These IR spectra are essentially identical, showing that the polyimide decomposed during the 400°C cure despite being stable in bulk form up to 450°C.

The XPS spectra in Figure 6-17 verify the IR results. The XPS survey of the 100 Å film cured at 250°C shows the typical ratio of C, N, and O bands. However, with the additional 400°C cure, the surface has an XPS spectrum like that of oxidized chromium.

SUMMARY

The IR and XPS results obtained in this work fit trends established by previously published data. Gold was shown to be inert during the curing of the polyimide. The results for chromium indicate it behaves more like gold in that no significant changes are observed in the IR or XPS spectra. Kelley *et al* [4] proposed this may be caused by the formation of a tight oxide layer between the polymer and the chromium, preventing diffusion of chromium ions into the polyimide. The results obtained for this thesis on high temperature curing of polyimide/chromium structures, considered with the results presented by Anderson *et al* [1] for polyimide curing and degradation on

Figure 6-16 IR Analysis of Cure Temperature Effect on 100 Å PI/Cr Structure

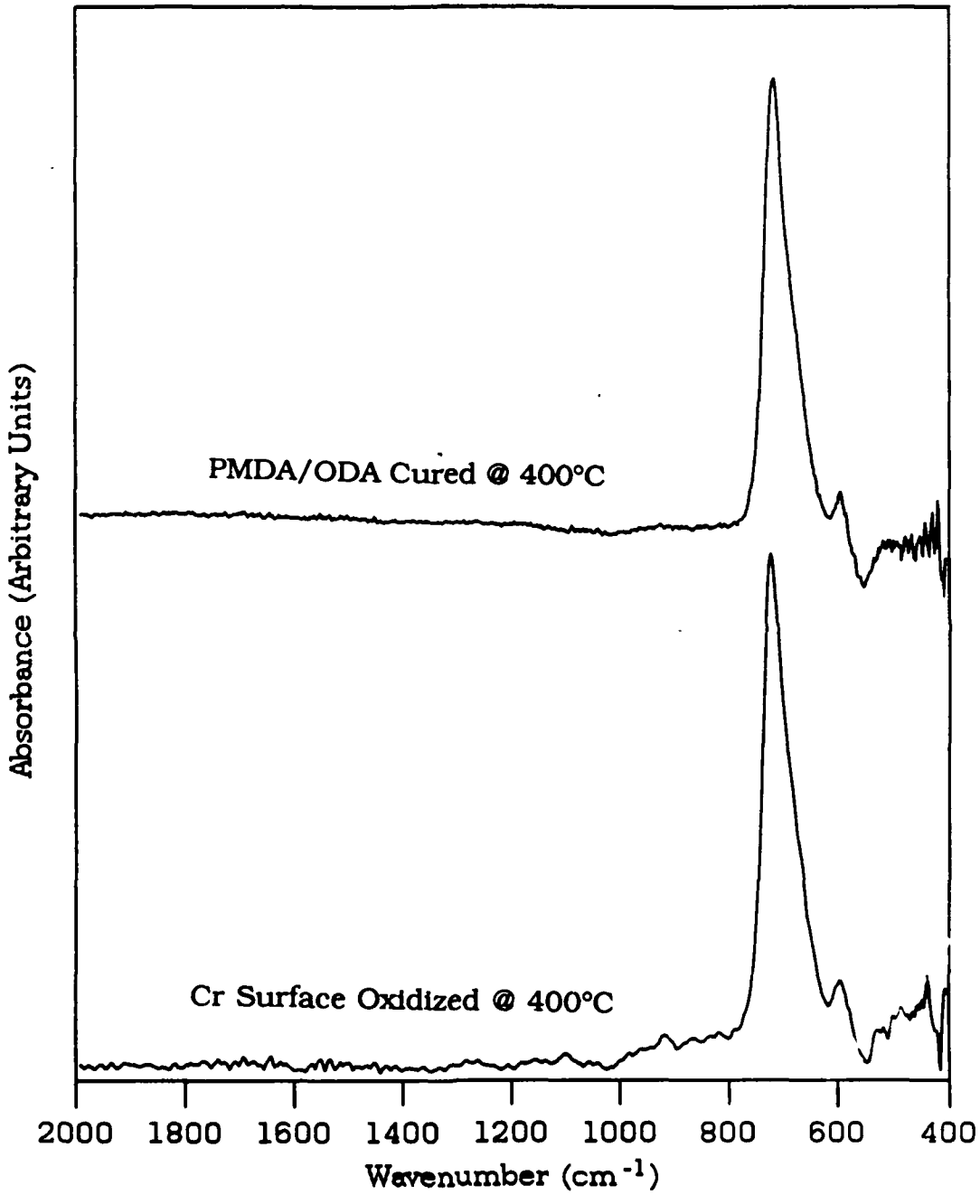

Figure 6-17. XPS Analysis of Cure Temperature Effect on 100 Å PI/Cr Structure

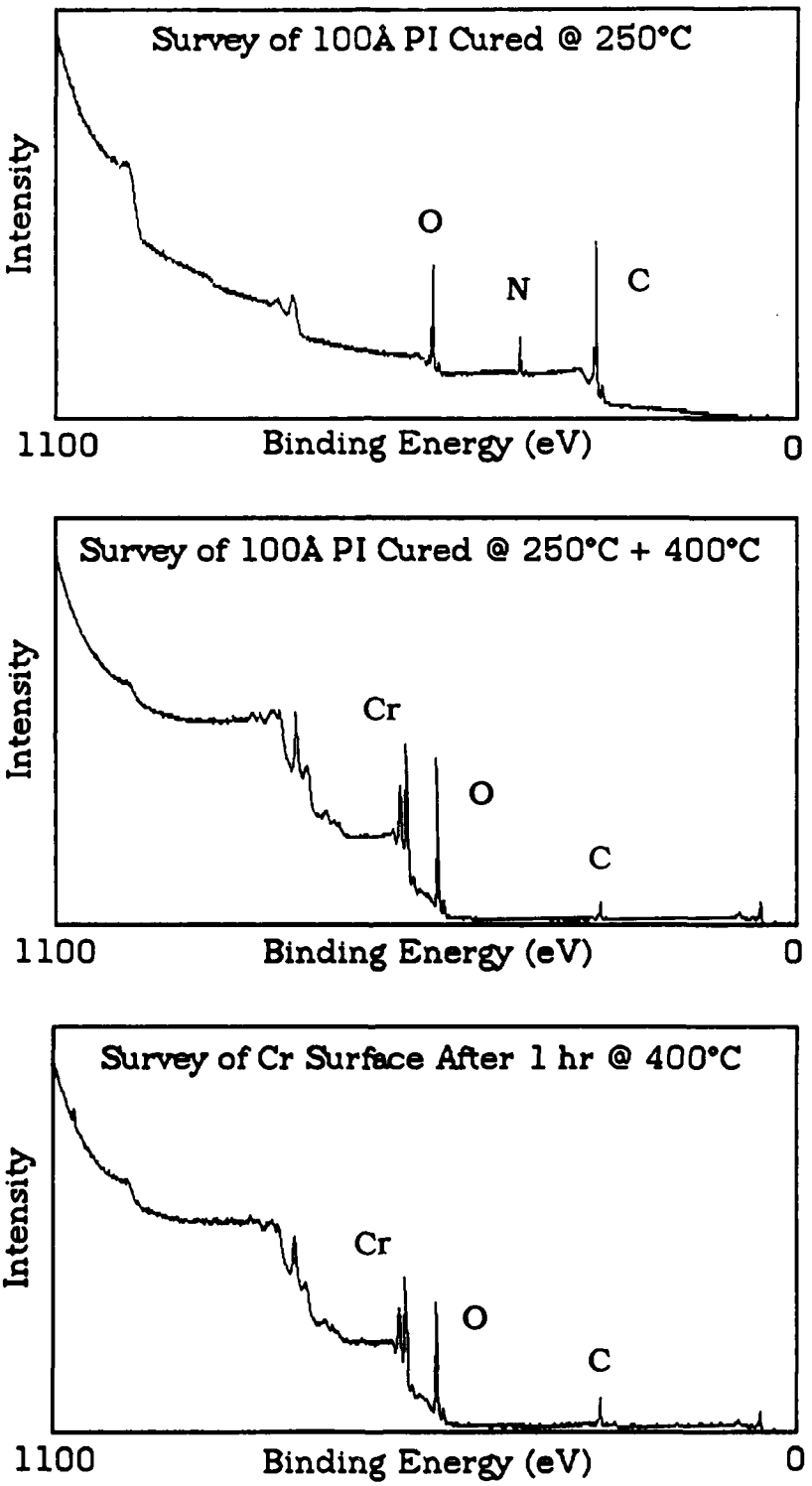

aluminum, suggest reaction may be occurring and is a function of the sample's thermal history. The polyimide at the interface is apparently less stable than the 450°C reported for bulk material.

The most significant changes were observed for the polyimide/copper system. IR peaks obtained for this system occurred in the same regions as those reported by Kelley *et al* [4] for thicker polyimide films. While Kelley *et al* [4] suggest no degradation occurs with nitrogen curing, the data presented here indicates the same processes are occurring, only at a slower rate in the nitrogen environment. The polymer itself can be a source of the oxygen for the reaction, and Kowalczyk *et al* [6] demonstrated that solvent can aid in transporting copper precipitates into the polyimide and expose fresh copper for reaction. Again, the data indicates the copper lowers the polyimide decomposition temperature below that reported for bulk polyimide. Based upon the IR and XPS data the copper interacts with the polyimide at the imide linkage.

REFERENCES

[1] S.G. Anderson, H.M. Meyer, III, Lj. Atanasoska, and J.H. Weaver, "Dynamics of Polyimide Curing and Degradation: An *in situ* X-ray Photoemission Study," *J. Vac. Sci. Technol.* , **A6 (1)**, 38-43 (1988).

[2] H.M. Meyer,III, S.G. Anderson, L.J. Atanasoska, and J.H. Weaver, "X-ray Photoemission Investigations of Clustering and Electron Emission, Injection, and Trapping at the Gold/Polyimide Interface," *J. Vac. Sci. Technol.*, **A6 (1)** , 30-37 (1988).

[3] L. Jordan, P.N. Sanda, J.F. Morar, C.A. Kovac, F.J. Himpsel, and R.A. Pollak, "Synchrotron-radiation Excited Carbon 1s Photoemission Study of Cr/Organic Polymer Interfaces," *J. Vac. Sci. Technol.*, **A4 (3)**, 1046-1048 (1986).

REFERENCES (continued)

[4]K. Kelley, Y. Ishino, and H. Ishida, "Fourier Transform IR Reflection Techniques For Characterization of Polyimide Films on Copper Substrates," *Thin Solid Films*, **154**, 271-279 (1987).

[5]R.M. Tromp, F.LeGoues, and P.S. Ho, "Interdiffusion at the Polyimide-Cu Interface," *J. Vac. Sci. Technol.*, **A3 (3)**, 782-785 (1985).

[6]S.P. Kowalczyk, Y.H. Kim, G.F. Walker, and J. Kim, "Polyimide on Copper: The Role of Solvent in the Formation of Copper Precipitates," *Appl. Phys. Lett.*, **52 (5)**, 375-376 (1988).

CHAPTER 7

CONCLUSIONS AND RECOMMENDATIONS

There is a fundamental difference in the processes which occur during the imidization of polyimide on metal and during the deposition of metal onto cured polyimide. Most previous work studied *in situ* metal depositions onto cured polyimide surfaces. Fewer results have been published on the curing of polyamic acid on metals. The work in this area by Kelley *et al* [1] and Kowalczyk *et al* [2] were significant in establishing some background for the polyimide/copper interface. In the work presented here, the complementary infrared (IR) and x-ray photoelectron spectroscopies (XPS) provided further insight into the chemical nature of the interface. The transmission electron microscopy work by Kowalczyk *et al* [2] was useful in interpreting the IR and XPS results for the polyimide/copper system. In addition to the polyimide/copper system, this thesis studied the chemical processes at the polyimide/gold and polyimide/chromium interfaces.

The experimental work showed that it is possible to collect IR spectra for polyimide films as thin as 34 Å. The technique required the use of reflection/absorption or internal reflection techniques to obtain spectra of thin films with an acceptable signal-to-noise ratio. The reflection/absorption technique provided the better spectra.

The IR spectra showed little interaction for gold and chromium systems with the 250°C cure; however, significant changes were

observed with copper. The chromium system did appear affected by higher cure temperatures.

The XPS data was also used to study the chemical changes which occurred with thinner films. It was very useful in verifying the lack of polyimide on the chromium surface following high temperature cure. Curve fitting was done to consider the changes in contributing chemical structures as the interface was approached. As with the IR results, the most significant changes were seen for the polyimide/copper system. The XPS results indicated that degradation of the polyimide occurred, contrary to the interpretation presented by Kelley *et al* [1] for polyimide cured on copper in a nitrogen environment. It was noted during the curve fitting process that the fit is very dependent on initial component estimates. For example, in some cases additional peaks could have been used to increase the fit in one region (i.e., indicating a new chemical structure), while not really increasing the overall fit of the curve.

The XPS and IR data suggest the need to characterize the morphology of the interface by transmission electron microscopy (TEM). Several of the early *in situ* experiments, in which metals were deposited on cured polyimide surfaces, developed extensive XPS chemical characterization of the interfaces. However, to fully understand the physical processes occurring at the interface, transmission electron micrographs were required. In the case of polyimide being imidized on copper, Kowalczyk *et al* [2] obtained micrographs which revealed the effect of solvent on the interfacial characteristics. Their work was very useful in interpreting the results

of this work, and similar TEM studies must be done to determine how different metals react during polyimide curing.

The TEM micrographs could be used to discern how chromium behaves when polyimide with solvent is imidized on it. It remains to be determined whether a stable interface is obtained as found with *in situ* depositions onto cured polyimide surfaces. or whether the polar solvent causes a process similar to that found for copper. These same questions should be studied for any of the interfaces found in polyimide applications.

Further work should be conducted to more closely explore the time/temperature/metal effects on the observed thermal stability of the interface. As previously stated, the imidized structure is stable up to 450°C in bulk form. In these studies polyimide at the interface was much less stable, showing indications of decomposition at temperatures as low as 250°C. The observed temperature sensitivity was a strong function of the metal at the interface. Copper provided the most decrease in stability, while gold had the least effect.

The solvent variable should also be considered in future research. While it is now known that the polyimide/copper interfacial properties are determined by the presence of solvent, further work must be conducted to determine the role of this variable in formation of other interfaces.

Future IR work needs to utilize the IR regions containing metal-oxygen, metal-carbon, and metal-nitrogen bonds. Since these regions are in the lower wavenumber region, techniques need to be developed to obtain spectra in this region with good signal-to-noise ratios. This

work showed the low wavenumber region is the most difficult to collect for thin films.

From a technique point of view, it may be useful to explore the possibility of depositing polyimide on an internal reflection element, with subsequent metal deposition. The element would have to be carefully chosen for both the optical properties and the thermal stability required to withstand polyimide curing. A variable angle IRE may also be useful for future work, since it allows various depths within the sample to be characterized without changing the sample. This type of depth profiling is not possible with the fixed angle plates or as easily implemented with reflection/absorption studies.

The experimental data collected on the interfaces formed between the PMDA/ODA polyimide and chromium, copper, and gold indicate the metals interact with the polyimide structure in a complex manner during the imidization process. Particularly notable was the observed temperature sensitivity of the polyimide at the interface when compared to the stability of bulk material. Further research needs to be conducted to look more closely at the time, temperature, and metal effects on the properties of polyimide/metal interfaces. In general, future research needs to characterize the process of polyimide-on-metal curing to the extent already accomplished for the reverse structure.

REFERENCES

[1]K. Kelley, Y. Ishino, and H. Ishida, "Fourier Transform IR Reflection Techniques For Characterization of Polyimide Films on Copper Substrates," *Thin Solid Films*, **154**, 271-279 (1987).

REFERENCES (continued)

[2]S.P. Kowalczyk, Y.H. Kim, G.F. Walker, and J. Kim, "Polyimide on Copper: The Role of Solvent in the Formation of Copper Precipitates," *Appl. Phys. Lett.*, **52 (5)**, 375-376 (1988).